

Thermal expansion coefficient, scaling, and universality near the superfluid transition of ^4He under pressure

K. H. Mueller*

Institut für Festkörperforschung, Kernforschungsanlage, 517 Jülich, West Germany

Guenter Ahlers†

Bell Laboratories, Murray Hill, New Jersey 07974

F. Pobell

Institut für Festkörperforschung, Kernforschungsanlage, 517 Jülich, West Germany

(Received 26 April 1976)

Experimental results for the isobaric-thermal-expansion coefficient β_p of pressurized ^4He near the superfluid transition temperature T_λ are reported. Near T_λ , β_p is an asymptotically linear function of the specific heat at constant pressure C_p . Therefore these measurements yield some of the same critical-point parameters as those derivable from C_p . The measurements were made with high-temperature resolution over the range $2 \times 10^{-5} \leq |t| \equiv |T/T_\lambda - 1| < 7 \times 10^{-2}$, along nine isobars. They span the pressure interval $5 \lesssim P \lesssim 30$ bar. A new experimental technique was employed which yielded a temperature resolution of two parts in 10^7 and a pressure stability of 1×10^{-7} bar. The results for each isobar were fitted with the equation $\beta_p = (A/\alpha)t^{-\alpha}(1 + Dt^x) + B$ above T_λ , and with the same expression with primed coefficients below T_λ . When the amplitudes D and D' of the confluent singularity are assumed to be equal to zero (i.e., the data are fitted with a pure power law), the leading exponents are pressure dependent and vary from 0.00 at low P to 0.06 at high P . This analysis also yields $B' > B$. The inequality between B and B' , and the pressure dependence of α and α' , are contrary to the predictions of the phenomenological and renormalization-group theories of critical phenomena. When D and D' are permitted to assume nonzero values, it is statistically allowed by the data to impose the theoretically predicted relations $\alpha = \alpha'$, $x = x'$, and $B = B'$ as constraints in the analysis. With these constraints, and the value of x chosen to be equal to 0.5, we obtain pressure-independent (universal) amplitude ratios and leading exponents, as expected from theory. Their values are $\alpha = \alpha' = -0.026 \pm 0.004$, $A/A' = 1.11 \pm 0.02$, and $D/D' = 1.29 \pm 0.25$. Similar results are obtained when x is chosen to be equal to 0.4 or 0.6. The result for α is consistent with that derived previously from specific-heat measurements. The universal A/A' is contrary to the previous report of a pressure-dependent specific-heat amplitude ratio. Using thermodynamic relations, we compare our β_p results directly with the C_p measurements. For $P \lesssim 15$ bar the agreement is excellent; but at the higher pressures there are small but significant differences of unknown origin.

I. INTRODUCTION

The superfluid transition of liquid helium has been investigated in recent years in great detail and with high precision¹ in order to test theoretical predictions pertaining to continuous phase transitions. The results of those studies have been compared with predictions of scaling,² of universality,³ and of the renormalization-group theory of critical phenomena.⁴ These theories predict that exponents, and certain dimensionless amplitude ratios, which describe the singularities of various properties near critical points, are universal in the sense that they depend only upon such general properties of the system as its spatial dimensionality d , and the number of degrees of freedom n (spin dimensionality) of its order parameter. This concept of universality received strong support from a variety of experiments,^{1,5} although there appear to be some experimental results which contradict this theoretical prediction.^{6,7}

For the superfluid transition, one has $n=2$ because the order parameter is complex. Since neither n nor d (nor any other known relevant property of the system) change as the pressure of the fluid is varied, one expects from renormalization-group theory that critical-point parameters such as exponents and certain amplitude ratios should be constant along the entire λ line. Nonetheless, recent measurements of the specific heat of ^4He near T_λ yielded an amplitude ratio A/A' of the leading singular part of C_p which depended upon the pressure P .⁷ Since those results disagree with the predicted universality, the present work was undertaken with the intention of providing a second measurement of A/A' by another independent experimental method. We measured the isobaric thermal expansion coefficient β_p of ^4He near T_λ for $2 \times 10^{-5} \lesssim |t| < 7 \times 10^{-2}$ and for $5 \lesssim P \lesssim 30$ bar. Here $t \equiv T/T_\lambda - 1$ and P is the pressure. Using the thermodynamic relations, one can show that β_p is a linear function of C_p sufficiently near T_λ (see

below).^{1,7} Therefore the same amplitude ratio A/A' and the same critical exponents α and α' can be derived either from β_P or from C_P . Our results for β_P are thermodynamically consistent within expected experimental uncertainties with the specific-heat results⁷ for pressures $P \lesssim 15$ bar. However, there exist small but significant inconsistencies between the two sets of data at the higher pressures which increase with pressure and with approach towards T_λ .

We analyzed the results for β_P by fitting them to the function⁸

$$\beta_P = (A/\alpha)|t|^{-\alpha}(1+D|t|^x) + B \quad (1.1)$$

for $T > T_\lambda$, and to the same function with primed coefficients for $T < T_\lambda$. In the analysis of measurements near critical points, it is often assumed that the amplitudes D and D' of the confluent singularity in Eq. (1.1) are negligibly small. Initially, we therefore also made this assumption, although there is of course no particular justification for doing so. The fit to the remaining pure power law yields exponents α and α' which depend significantly upon the pressure and vary from about 0.00 for small P to about 0.06 near the melting line ($P \cong 30$ bar). This analysis also gave values of B' which were consistently and significantly larger than those of B . From renormalization-group theory it is expected that $B = B'$,⁹ and that $\alpha = \alpha'$ and independent of the pressure. We do not regard these departures from the theoretical predictions to be real, however, and will show that full agreement with theory can be obtained by permitting the amplitudes D and D' of the confluent singularity in Eq. (1.1) to assume nonzero values. When the terms $D|t|^x$ and $D'|t|^{x'}$ are included in the data analysis, it is possible to have $B = B'$ and $\alpha = \alpha'$, as expected from theory, without causing statistically significant departures of the data from the fitted function. The data and Eq. (1.1) with these constraints, and with $x = x' = 0.5$, yield $\alpha = \alpha' = -0.026 \pm 0.004$, $A/A' = 1.11 \pm 0.02$, and $D/D' = 1.29 \pm 0.25$. These three parameters within their experimental uncertainty are independent of pressure along the entire λ line, as expected from theory. The value of $\alpha = \alpha'$ is in agreement with that given by the specific-heat measurements.⁷ The results for C_P also had revealed already that the scaling prediction $\alpha = \alpha'$ was satisfied by the data only when nonzero values of D and D' were allowed in the data analysis. But the pressure dependence of A/A' which was indicated by the C_P results is *not* confirmed by the present data for β_P . Although we have been unable to find an explanation for the discrepancy, we are inclined to believe that the previous result should be regarded as spurious and that the universal A/A' , based

upon β_P , reflects the true behavior of the system. Although we have no rational basis for this belief, we do call attention to the fact that the present measurements give β_P directly, whereas the results for C_P are not based on direct measurements. Instead, C_P was derived via thermodynamic relations from the measured heat capacity C_V at constant volume.

In Sec. II we describe the principle of a new high-precision technique which was used to measure β_P . In Sec. III we discuss the cryogenic and electronic aspects of our experiment and the experimental procedure. Section IV contains the analysis performed to calculate β_P from the raw data, and a discussion of the experimental errors. The results are presented in Sec. V. Section VI contains the discussion, and in particular a comparison of our results for critical exponents and amplitude ratios with predictions of scaling, universality, and renormalization-group theory. A summary of our results is provided in Sec. VII.

A brief report on this work has been given previously.¹⁰

II. PRINCIPLE OF THE EXPERIMENTAL METHOD

Thermal-expansion coefficients of liquids usually have been determined either by measuring volume changes in a pycnometer, or by measuring dielectric constant changes in a capacitor. Our measurements were made by a new technique which is capable of very high resolution, and which is especially suited for investigations near the λ line. Our method reduces the experimental procedure to a high-precision regulation of the sample pressure, and the measurement of temperature changes. It avoids the direct measurements of changes in volume or dielectric constant.

The principle of the method is demonstrated in Fig. 1. Part of the helium used for the measurements occupies the "sample" volume v_s , and the remainder is in the "hot" volume v_h . The experiment is performed at constant pressure, and at constant total volume ($v_s + v_h$). The temperature T_s of the sample is held near T_λ , where the expansion coefficient has a large negative value and is strongly temperature dependent. The volume v_h is connected to v_s via a small capillary. The capillary diameter is small enough to result in a tolerable heat transport, and yet large enough to yield only negligible pressure gradients. The temperature T_h of the hot volume is kept between 2.5 and 4 K, and is free to change in this range where the expansion coefficient is positive and has a small regular temperature dependence.¹¹ The pressure P_s is measured by a capacitance strain gauge,¹² which is attached to the sample volume. Any devi-

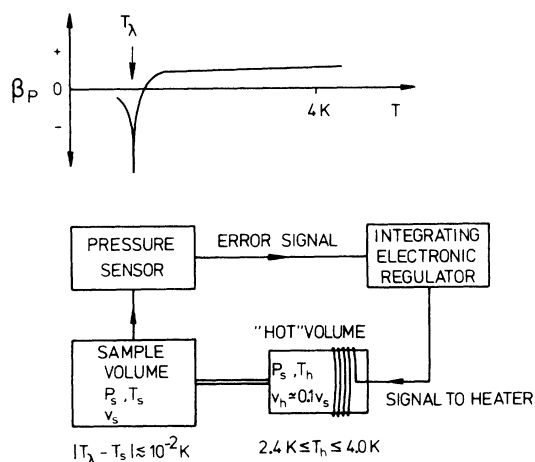


FIG. 1. Schematic representation of the experimental method.

ation of P_s from a reference pressure produces an error signal which is used to change the temperature T_h so as to return P_s to its reference value. Any change ΔT_s of the sample temperature therefore has to be compensated by a change ΔT_h of the temperature of the hot volume if the pressure is to stay constant. The amount of liquid flowing out of (or into) the sample volume due to a temperature change ΔT_s at constant P has to be allowed to flow into (or out of) the hot volume by changing the temperature of v_h by an appropriate amount ΔT_h . Thus, the isobaric temperature change ΔT_h is proportional to the isobaric molar volume change ΔV of the fluid in v_s . The thermal-expansion coefficient $\beta_{P,s}$ of the liquid in the sample is then given by

$$\beta_{P,s} = \lim_{\Delta T_s \rightarrow 0} -\beta_{P,h} \frac{\Delta T_h N_h}{\Delta T_s N_s}, \quad (2.1)$$

where $\beta_{P,h}$ is the isobaric thermal-expansion coefficient of the fluid in the hot volume, N_i is the number of moles in the chamber i , and N_h/N_s can be determined from the measured volume ratio v_h/v_s . The data then consist of readings of the temperature changes ΔT_h of the hot volume which are caused by various regulated isobaric temperature changes ΔT_s of the sample volume. By choosing $v_s \approx 10v_h$, we have under most circumstances $|\Delta T_h| > 10|\Delta T_s|$ because usually $|\beta_{P,h}| < |\beta_{P,s}|$. Therefore, the accuracy of the data depends essentially only on the resolution with which ΔT_s can be measured, and on the pressure regulation. The requirement for the latter is rather severe. For a thermal-expansion coefficient of 0.1 K^{-1} and a compressibility of 10^{-2} bar^{-1} , which are typical for ^4He near T_λ , the pressure resolution corresponding to a temperature resolution of 10^{-7} K is

10^{-6} bar . With the experimental apparatus to be discussed in Sec. III we obtained a pressure regulation of typically 10^{-7} bar , and a resolution in the temperature measurement of $\delta T/T \approx 1 \times 10^{-7}$.

A particular advantage of our method is that we use a closed system at low temperatures, thus eliminating any possibility of mass exchange with hotter parts of the apparatus. A further positive aspect is that we placed critical components of our measuring systems, such as pressure transducers and reference resistors, on the sample chamber or at another well-regulated low temperature. Under these circumstances, thermal-expansion effects in the constituent parts are small, and extremely high stability and reproducibility can be achieved.

III. DETAILS OF THE APPARATUS AND THE PROCEDURE

A. Cryogenic apparatus

1. General arrangement

The main part of the cryogenic apparatus is shown in Fig. 2. It is contained in a vacuum can which is surrounded by a helium bath at 4.2 K. The first stage inside this can is a continuous ^4He refrigerator¹³ with a ^4He volume of about 5 cm^3 . The operating temperature of this refrigerator is about 1.35 K and is constant to $\pm 3 \text{ mK}$. In order to

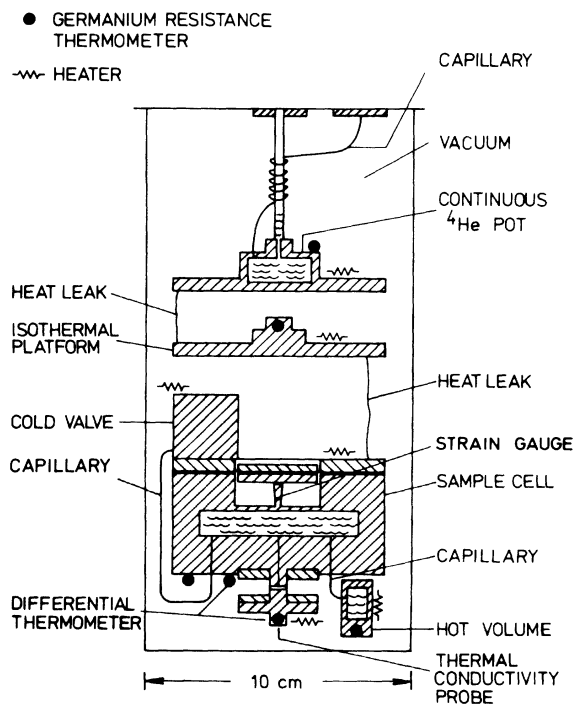


FIG. 2. Schematic diagram of the low-temperature portion of the apparatus.

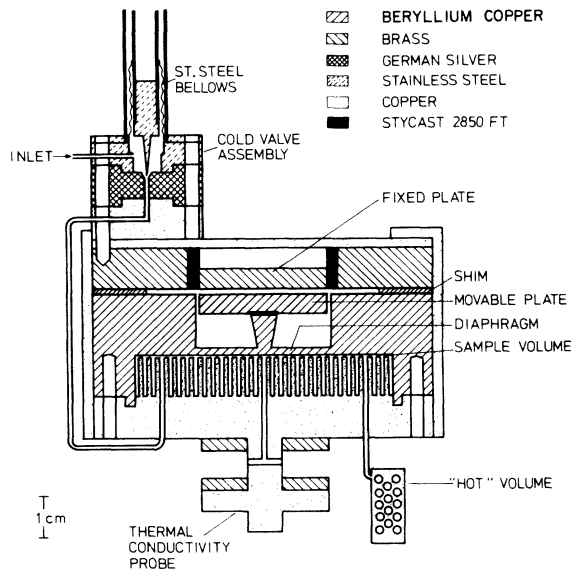


FIG. 3. Schematic diagram of the details of the sample cell and hot volume.

improve the thermal stability of the sample cell, a copper disk is used as an isothermal platform¹⁴ between the 1.35-K stage and the sample. The isothermal platform temperature is regulated at about 1.5 K with a heater, and a germanium thermometer in an ac bridge, to $\pm 8 \mu\text{K}$. A thin copper wire and the necessary structural members provide a heat leak typically of 1×10^{-4} W from the isothermal platform to the ^4He pot.

All wires and capillaries that lead to the sample cell are carefully heat sunk at the top flange of the vacuum can (4.2 K), at the ^4He pot (1.35 K), and at the isothermal platform (1.5 K), before they are connected to their final destination. Radiation heat input is reduced by radiation shields in all tubes leading to the vacuum can, and around the sample cell.

In Fig. 3, more details of the central part of the apparatus are shown. The sample volume and hot volume can be filled through a valve with liquid helium. The valve is at the same temperature as the sample volume. It is actuated mechanically from outside the low-temperature part of the apparatus. It has a German silver seat with a 0.1-cm-diam hole, and a stainless-steel needle with a 3° taper. A copper capillary (0.02-cm i.d. and 0.1-cm o.d.) leads from the valve to the sample cell. After filling the sample and hot volumes, the valve is closed and the filling capillary (stainless steel, 0.08-cm i.d. and 0.01-cm wall thickness) above the valve is evacuated. Emptying this capillary is aided by raising its temperature with a heater wound onto the top half of the stainless-

steel bellows of the valve. The stainless-steel tubes which lead to the German silver seat and to the stainless-steel needle of the valve are heat sunk with copper braids to the 4.2-K ^4He bath, to the 1.35-K ^4He stage, and to the isothermal platform. A heat leak from the sample cell to the isothermal platform of typically 5×10^{-5} W is provided by the tubes of the cold valve. This heat leak is of course very constant in time because of the constancy of the isothermal platform temperature.

2. Sample cell and hot cell

The top part of the sample cell contains the movable diaphragm of the pressure transducer (see below) and is made of beryllium-copper. The lower part of the cell is made of a single piece of copper. The sample volume consists primarily of 0.1-cm-wide and 1-cm-high grooves, which are cut into the lower copper part of the cell. Connected to the sample volume via a capillary is the hot volume. This volume is made of a copper piece into which 14 holes of 0.2 cm diameter and 3.4 cm length are drilled. Everywhere in the sample the liquid is no more than 0.05 cm away from a copper wall. In the hot volume this maximum distance is 0.1 cm. This design reduces thermal relaxation times of the system to less than 10 sec even for He I.

The hot volume v_h is approximately equal to 10% of the sample volume v_s . This volume ratio, and the relative size of the expansion coefficient of ^4He near T_λ and at high temperatures, assure that the temperature change ΔT_h of the hot volume will be an order of magnitude larger than the temperature change ΔT_s of the sample volume in a typical measurement [see Eq. (2.1)]. The large ΔT_h can be measured easily with a relative error considerably smaller than that of ΔT_s . The random uncertainty of a measured value of β_p , therefore, is determined primarily by the temperature resolution of 2×10^{-7} K of T_s .

The stainless-steel capillary which connects the sample and hot volumes has a 0.035-cm o.d., a 0.01-cm i.d., and is 4 cm long. Its volume is 3×10^{-4} cm³, which is only $2 \times 10^{-3}\%$ of the total sample volume. Changes in temperature gradients along this capillary will therefore have a negligible effect upon the density of the fluid in v_h or v_s .

When T_s is less than T_λ , part of the capillary between v_h and v_s will contain superfluid helium in a temperature gradient. The heat carried by the superfluid flow is limited by dissipative processes such as the so called "mutual friction," and can be estimated from detailed independent experimental measurements¹⁵ on a similar system to be about $30 \mu\text{W}$ when T_s is 0.01 K below T_λ . This heat cur-

rent vanishes when $T_s = T_\lambda$. The heat input to the sample volume is balanced by part of the heat leak to the isothermal platform. When $T_s > T_\lambda$, heat losses from the hot volume are very small because the fluid in the capillary between v_h and v_s is He I. Under these circumstances it is difficult to regulate T_h ; and we therefore deliberately introduced a heat leak of typically 3×10^{-5} W between the hot volume and the isothermal platform.

The total volume $v_h + v_s$ was determined by filling it with liquid helium at a known pressure and temperature, and then evaporating this liquid into calibrated glass bulbs at room temperature. We find

$$v_s + v_h = 16.50 \pm 0.16 \text{ cm}^3. \quad (3.1)$$

The ratio v_h/v_s was determined by adjusting the temperature of the two volumes to approximately the same temperature near 2.4 K. Here β_p is a regular, slowly varying function of T , and known from the measurements of Elwell and Meyer.¹¹ With the pressure held constant, measurements of T_h and T_s were made just as for the data near T_λ (details of the procedure are given below), but in this case the expansion coefficient of the fluid in both volumes is known and it is possible to calculate the volume ratio. The effect of possible errors in the measurements of Elwell and Meyer is minimized by having $\beta_{p,h} \cong \beta_{p,s}$; for if the two expansion coefficients were equal, one would have $v_h/v_s = \Delta T_s / \Delta T_h$. We measured v_h/v_s near the maximum and minimum pressures of the experiment, and found the same ratio within the resolution of 0.1%. This is consistent with our estimate of the flexure of the pressure sensor diaphragm, which corresponds to a change in v_s of 0.05% due to a pressure change of 30 bar. We find

$$v_h/v_s = 0.096 15 \pm 0.000 10. \quad (3.2)$$

3. λ -point detector

We detected the superfluid transition by establishing the temperature at which thermal resistance in the liquid is first noticeable.¹⁶ For this purpose, a small thermal-conductivity probe is attached to the bottom of the main sample¹⁴ (see Fig. 3). Some of the fluid can flow into this λ -point detector through a 0.1-cm-diam hole in the sample-cell bottom. The thermal-conductivity cell is 0.1 cm high, has a 0.58 cm diameter, and has stainless-steel walls of 10^{-2} cm thickness. Power generated (typically 10^{-7} W) in a heater and a thermometer which are attached to the thermal-conductivity cell bottom has to flow primarily through the 0.1-cm-thick fluid layer. It produces a temperature difference across the λ -point detector when $T > T_\lambda$, and the thermal resistance of

the fluid is nonzero. This temperature gradient is detected by comparing the thermometer at the bottom of the probe with another on the main sample cell. It is possible by this method to determine T_λ in the λ -point detector to within the resolution of the main thermometer on the sample volume, or typically to $\pm 2 \times 10^{-7}$ K. The λ point in the main sample is at a slightly higher temperature because of the effect of the gravitational field.¹⁷ The measurements of T_λ are easily corrected for this gravity effect, and our final values pertain to the middle of the sample volume which is located 2.3 cm above the λ -point detector.

In the immediate vicinity of T_λ , the temperature difference across the λ -point detector provides a very sensitive measurement of the temperature of the main sample. Temperature changes of 10^{-9} K can be resolved over the 10^{-7} -K temperature interval where the He II-He I interface moves vertically through the thermal-conductivity cell.¹⁶ We have utilized this extremely high sensitivity to regulate the sample temperature in this temperature interval to better than 10^{-8} K. With the sample temperature held constant, we were then able to evaluate the performance of the pressure regulation system and of the hot-volume thermometer system (see Sec. III C).

4. Thermometers and heaters

Six heaters and six thermometers at various points of the low-temperature apparatus (see Fig. 2) made it possible to regulate and measure the temperatures of the various stages. Heaters were generally made of 0.01-cm-diam Karma wire, had resistances of several k Ω , and were attached to various points using GE 7031 varnish. We used encapsulated germanium thermometers¹⁸ which were pushed into holes containing Apiezon type *N* grease. They were all model CR 2500L, except for the one on the sample volume which was model CR 1000.¹⁸ All thermometer leads were thermally attached to the substrate whose temperature was to be measured.

5. Pressure gauge

The pressure gauge is an integral part of the sample cell. It is a capacitive pressure transducer of the type employed by Straty and Adams.^{12,19} An elastically deformable diaphragm is part of the beryllium-copper top piece of the sample cell (see Fig. 3). It is 0.15 cm thick and has a diameter of 3.2 cm. A 3-cm-diam plate is glued rigidly with Stycast FT 2850 epoxy to a post on the center of the diaphragm (see Fig. 3). Any diaphragm deflection is therefore transmitted to this plate; but the plate is electrically isolated from its surround-

ings. A second plate of 3.0 cm diameter is glued similarly in a *fixed* position and also electrically isolated. A three-lead method can therefore be used to determine the capacitance between the plates. This capacitance is a measure of the plate separation, and therefore of the pressure in the cell.

Both of the capacitor plates are lapped to a flat mirror finish. The gap between them is adjustable by means of shims of various thicknesses to provide maximum sensitivity at a particular operating pressure. A typical gap width was 30 μm and yielded a pressure sensitivity of 10^{-7} bar with the capacitance resolution of one part in 10^8 . With the cell evacuated, the pressure gauge had the negligible temperature dependence $(1/\Delta T)(\Delta C/C) = 1.8 \times 10^{-6} \text{ K}^{-1}$ over the range $1.6 \leq T \leq 2.6 \text{ K}$.

The capacitive pressure gauge was calibrated with an accuracy of ± 0.03 bar by comparing it with a Heise bourdon-tube gauge.²⁰

B. Electronics

Our method of measuring the thermal-expansion coefficient required the precise measurement or control of three parameters. These are the liquid pressure, and the temperatures of the sample and the hot volume.

Both temperatures were measured by determining the resistance of calibrated germanium thermometers. This was done by using an alternating-current bridge method, which to a large extent has been described elsewhere.¹⁷ However, some of the details of the thermometry have been optimized over the intervening years.^{7,14,19} We show a schematic diagram of the circuit in Fig. 4. Metal film resistors²¹ were used as standards in the bridges. They were mounted in the cryostat on the isothermal platform in order to eliminate any effects due to their already small temperature coefficient and to reduce the size of the Johnson noise. Their resistance changed typically

by 2% upon cooling from 300 to 2 K. Temperature stabilization of the ratio transformers was not considered necessary because their transfer characteristics are virtually independent of the laboratory temperature. They contribute little to the noise because they are in principle nondissipative devices. One frequently encountered problem in high-resolution thermometry is the effect of changes in the lead resistance upon the bridge balance which might be associated with long-term changes in temperature gradients along the leads in the cryostat. To first order, these changes tend to cancel even when only three leads are brought out of the cryostat. However, we used five leads for each thermometer, and operated the ratio transformers²² at a frequency near 35 Hz where their impedance was at least an order of magnitude larger than the resistance of the thermometers and reference resistors. This serves to further minimize the importance of lead-resistance changes. A much higher operating frequency was not considered desirable because it would increase the size of the out-of-phase signal due to any capacitive bridge unbalance. The out-of-phase signal was minimized by adjusting the variable capacitor shown in Fig. 4. The amplitude of the excitation signal from the reference oscillator of the lock-in detector²³ varied by less than 0.1%. This assured a time-independent power dissipation in the thermometers. It is important to maintain a constant thermometer power dissipation because we operated at maximum tolerable bridge power in order to maximize the temperature resolution. The self-heating of the temperature sensors above the temperature of the substrate was typically 10^{-4} K . With a power stability of about one part in 10^3 , temperature changes of 10^{-7} K can thus still be measured if the noise level of the bridge is sufficiently low. The gain stability of the lock-in detector was not a critical factor since measurements were nearly always taken close to a null condition and the precision to which the size of the out-of-balance signal had to be known was at most a few percent. Repeated checks on the sensitivity of the bridge system verified that this requirement was met. Drifts in the null position of the lock-in detector were always negligible.

Pressure measurements were made with the capacitance transducer described in Sec. III A 5. The capacitance was determined by a three-lead technique with a commercially available bridge²⁴ in a conventional guarded capacitor arrangement. Coaxial cables were used throughout. The internal arrangement of the capacitance bridge is essentially that of a ratio transformer, and a switch-selectable bank of standard capacitors which have

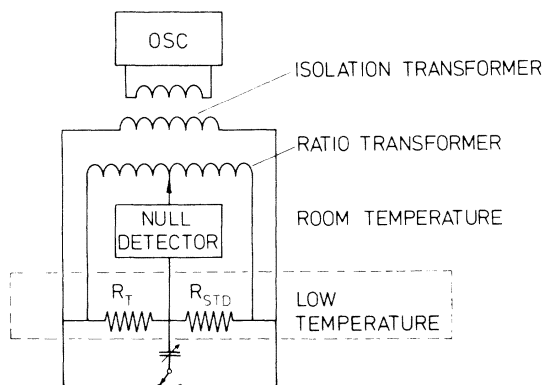


FIG. 4. Schematic diagram of the thermometry bridge.

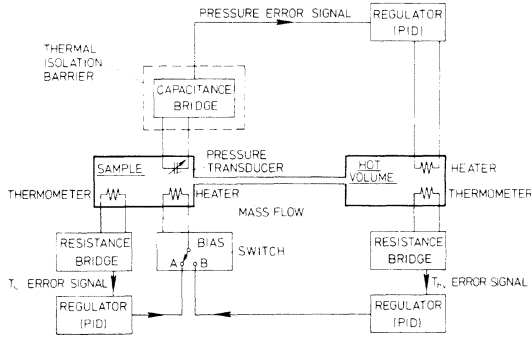


FIG. 5. Schematic diagram illustrating two possible modes of operation for the experiment. See text for details.

a temperature coefficient $(1/\Delta T)(\Delta C/C)$ of $(2-3) \times 10^{-6} \text{ K}^{-1}$. Since we wanted a stability of one part in 10^8 , it was necessary to regulate the temperature of these standard capacitors. They were already enclosed in a hermetically sealed metal container and thermally insulated. Therefore it was necessary only to provide a heater and thermometer to obtain a system suitable for regulation. A thermistor was used as temperature sensor, and its resistance was measured with a dc Wheatstone bridge. After suitable amplification a signal proportional to the deviation from a fixed temperature was provided to the heater. The thermal stability as measured with a second independent thermistor was $\pm 10 \text{ mK}$ long term (weeks) and $\pm 1 \text{ mK}$ over several hours. Thus, over the period of a set of measurements the standard capacitors were estimated to be stable to a few parts in 10^9 .

Each of the bridge circuits discussed in this section was used at some time in a regulation loop, which made it possible to maintain balance at any desired point. In order to obtain maximum accuracy and stability, each regulatory system included a feedback controller²⁵ which was capable of being adjusted to the frequency response of the cryogenic system so as to maximize the stability of the control loop.²⁶ The controller could maintain the integral of the out-of-balance signal at zero, thus eliminating entirely effects associated with the gain of the bridge null detector.

C. Performance and procedure

We always used the capacitive pressure gauge on the sample volume in a regulation loop to adjust the hot-volume temperature so as to keep the pressure of the fluid constant. However, for the temperature control of the sample volume, we had several different methods at our disposal and we used the one best suited for the purpose at hand.

Two of these are shown schematically in Fig. 5.

With the switch shown in Fig. 5 in the A position, the sample thermometer is used to provide power to the heater on the sample volume at a level sufficient to maintain the sample temperature T_s at a constant value. Although this would seem to be the most direct way of conducting the experiment, it is not the most advantageous one. The reason for this is that in some sense the sample thermometer, although it gives T_s most directly, has a lesser temperature resolution than other more indirect indicators of T_s . At a thermometer power level of $2 \times 10^{-8} \text{ W}$, the peak-to-peak noise on the sample thermometer is typically equivalent to 10^{-6} K . When the sample thermometer is used to regulate the sample temperature (switch position A in Fig. 5), this noise is converted into actual temperature fluctuations of about the same size. In the absence of pressure regulation, these temperature fluctuations would be accompanied by pressure fluctuations because of the nonzero expansion coefficient of the fluid. However, the pressure-regulation loop counteracts these pressure fluctuations by adjusting the temperature of the hot volume. Because of the relative size of the hot and sample volumes (see Sec. III A 2), the associated temperature fluctuations of the hot volume are at least an order of magnitude larger than the fluctuations of the sample temperature (see Sec. II). They are thus easily measurable with the hot-volume thermometer, and they confirmed that this mode of operation did indeed result in sample temperature fluctuations which had a peak-to-peak amplitude of typically 10^{-6} K .

In order to maintain the sample temperature at a more nearly constant value, we used an alternate method which is illustrated in Fig. 5 with the switch in position B. Under these circumstances, the hot-volume thermometer is used to provide power to the sample heater and to hold the sample temperature constant. Since the hot-volume thermometer under most conditions is at least an order of magnitude more sensitive to changes in T_s , the noise on T_h , equivalent to fluctuations in T_h of 10^{-6} K , will produce temperature fluctuations in T_s of less than 10^{-7} K . However, with this method of operation the system is unstable to large-amplitude perturbations of T_s . We therefore always used the system first with the switch in position A (Fig. 5) to obtain an approximate balance after a change in T_s , and then switched to position B to obtain the greatest possible stability of T_s and T_h .

Well above T_λ , there is a temperature T_0 where β_p vanishes. In the vicinity of T_0 , the hot-volume temperature becomes insensitive to changes in T_s . Under those circumstances, it became necessary to leave the switch (Fig. 5) in position A and to use

the sample thermometer to regulate T_s . But in that case, $T_s - T_\lambda$ is large and large increments ΔT_s can be used for the measurement. Therefore, it is no longer as important to hold T_s very constant.

The use of T_h for the regulation of T_s (switch position *B*, Fig. 5) requires that the hot-volume-thermometer system and the capacitive-pressure-gauge system are free from drifts and spurious changes at the level of resolution of one part in 10^7 or 10^8 of the measurements. Because of this non-trivial requirement, we used yet another method of holding T_s constant in order to test the stability and performance of the other bridges. We adjusted the sample temperature to such a value that the He II-He I interface was in the thermal-conductivity probe. As explained in Sec. III A 3, under these circumstances the λ -point detector is sensitive to changes of less than 10^{-8} K in T_s and can thus be used to regulate T_s at this level of resolution. With T_s regulated in this manner, and with T_h controlled by the pressure gauge, we monitored T_h and T_s with the two thermometers which were not involved in any regulation loop. The hot-volume thermometer was stable within its resolution as long as it was monitored (up to several hours). It was reproducible after thermal cycles of T_s away from and back again to T_λ . This implies of course not only the absence of drifts in the bridge used to monitor T_s , but also the absence of drifts in the pressure sensor and capacitance bridge. In order for this mode of operation to yield a constant T_h , it was necessary also to have a constant total amount of fluid in the system. We were therefore able to use it to ascertain with very high resolution that the cold valve had been properly closed and that there was no leak in the sample system. There were very slight changes in T_h from day to day, equivalent to changes in T_λ of perhaps 10^{-7} K. We do not know the cause of these changes; but they are not particularly surprising since the mechanical disturbances involved in transferring helium for instance can be expected to cause slight shifts in the pressure gauge capacitor. In any event, these changes from day to day are insignificant in relation to the measurements.

While regulating T_s with the λ -point detector, we discovered that unfortunately the thermometer used to monitor T_s was subject to measurable drifts.²⁷ These drifts never caused any problem in the determination of ΔT_s during a measurement of β_p because the time involved in this measurement is only of the order of 1 min; but the accurate determining of $T_\lambda - T_s$ required a frequent measurement of the thermometer resistance R_λ at T_λ . Usually, R_λ was determined after a set of 6-8 measurements of β_p had been completed.

D. Calibrations

The thermometers on the sample volume and the hot volume were calibrated on the 1958 ^4He vapor-pressure scale of temperatures²⁸ (T_{58}). For this purpose, ^4He exchange gas was put into the vacuum can (see Fig. 2), and the ^4He -bath vapor pressure was measured. For $T > T_\lambda$, calibration points were taken only after bath temperature decreases, and hydrostatic head corrections were made. Pressure measurements were obtained with a Barocel²⁹ measuring system which had been calibrated against a mercury manometer. In the temperature regions of interest for the sample and hot volume we believe that our temperature scale differs from T_{58} by no more than 1×10^{-3} K.

The temperature measurements consisted of values for the "bridge ratio" \mathcal{R} , which is equal to the settings of the ratio transformers in Fig. 4. The resistances R of the germanium thermometers at the calibration points were calculated on the basis of an adopted value R_{std} for the standard resistor, using the relation

$$R = R_{\text{std}} \mathcal{R} / (1 - \mathcal{R}). \quad (3.3)$$

When calculating a temperature from a measured bridge ratio, exactly the same value of R_{std} was used. For each thermometer, the calibration values of R , and the corresponding temperatures, were least-squares fitted to the equation

$$\log_{10}(T) = \sum_{i=0}^4 A_i [\log_{10}(R)]^i \quad (3.4)$$

over the temperature range $4.23 \geq T \geq 1.75$ K. Deviations from the fits generally did not exceed 1×10^{-3} K.

Our pressure scale was maintained on a Heise bourdon tube gauge²⁰ which had a pressure range of 0-32 bar and which could be read with a resolution of ± 0.02 bar. Before the measurements, the Heise gauge was calibrated against a dead-weight tester with an accuracy exceeding the resolution of the gauge. After the experiment, the calibration was checked by comparison with a precision manometer having an absolute accuracy of ± 0.04 bar. These calibrations revealed no changes in the pressure scale of the Heise gauge during the course of this work. We estimate that ambient pressure and temperature variations could introduce errors of ± 0.03 to ± 0.06 bar, depending on how frequently the gauge zero was determined. The uncertainties quoted below for P_λ are based upon these error considerations, and differ somewhat between the different runs.

The capacitive pressure transducer (see Sec. III A 5) was calibrated prior to a set of measurements on a particular isobar against the Heise

gauge. This was done by comparing the two at several pressures over about a 1-bar range which included the pressure of the isobar in question. Thereafter, the cold valve was closed, and the hot-volume temperature was adjusted to a value which yielded the desired sample pressure. The pressure was then determined from the capacitance of the pressure transducer and the calibration over the 1-bar range. This value of P is given as P_{λ_1} in column 1 of Table II.

In order to determine the sensitivity of the capacitive pressure transducer, a calibration against the Heise gauge was also obtained over a wider pressure range. Over the range 5–25 bar the data could be represented within ± 0.1 pF by

$$C = A_1 + A_2/(A_3 - P), \quad (3.5)$$

with $A_1 = 8.1069$ pF, $A_2 = 1812.7$ pF bar, and $A_3 = 33.602$ bar. We found the capacitance gauge to be stable over long time periods within the resolution of our calibration, provided that the pressure never exceeded the value at which the two plates touched. After such an overpressure, a new calibration was required. The isobar pressures based on Eq. (3.5) are given as P_{λ_2} in the second column of Table III, and agree within the estimated uncertainties with the values based on the individual calibrations over the narrow pressure ranges.

IV. DATA ANALYSIS AND ERRORS

A. Analysis

The measurements consist of a pair of values T_{h1}, T_{s1} for the temperatures of the hot volume and the sample volume before a temperature increment, and of a similar pair T_{h2}, T_{s2} after a temperature increment. The temperature change $\Delta T_s = T_{s2} - T_{s1}$ of the sample volume is of course isobaric because the pressure transducer which controls T_h senses the sample pressure P_s . The temperatures are derived from the corresponding thermometer bridge ratios as described in Sec.

III D. The initial calculation, leading to the determination of β_p , consists of determining $(\Delta\rho)_s/\Delta T_s$ and an appropriate mean temperature \bar{T}_s from these data. Here $(\Delta\rho)_s$ is the change in density of the fluid in the sample volume which is associated with ΔT_s . We use $\bar{T}_s = \frac{1}{2}(T_{s1} + T_{s2})$. Since the hot volume v_h , and the sum of the amount of fluid in v_h and in the sample volume v_s , remain constant during a measurement, one can show that

$$(\Delta\rho)_s = - (v_h/v_s)(\Delta\rho)_h, \quad (4.1)$$

where $(\Delta\rho)_h = \rho_{h2} - \rho_{h1}$. It remains to determine $(\Delta\rho)_h$.

For $T_s > T_\lambda$, it is clear that isobaric conditions prevail in v_h as well as in v_s because classical thermomolecular pressure gradients across the capillary connecting the two volumes are completely negligible. However, for $T_s < T_\lambda$, P_h will differ from P_s by an increment P_f due to the fountain pressure across the capillary. Nonetheless, we will assume that P_h is constant and neglect the effect upon $(\Delta\rho)_h$ of changes ΔP_f in P_f which are associated with temperature changes ΔT_s . Justification for this approximation is given in Appendix A. With the assumption of isobaric conditions in v_h , the data of Elwell and Meyer¹¹ (EM) for the molar volume V as a function of temperature at various pressures were used to determine

$$(\Delta\rho)_h = M/V_{h2} - M/V_{h1}. \quad (4.2)$$

Here V_{h2} and V_{h1} are the molar volumes of the fluid at the temperatures T_{h2} and T_{h1} , and $M = 4.0038$ g/mole is the molar mass of ⁴He.

In order to obtain a smooth representation of the EM data which made it possible to calculate even small changes in ρ , we least-squares fitted the molar volume data of EM to the equation

$$V(T) = \sum_{i=0}^4 m_i T^i \quad (4.3)$$

for a given isobar. The data did not deviate from the fitted function by more than ± 0.001 cm³/mole.

TABLE I. Coefficients of Eq. (4.3).

P (nominal) (bar)	T range (K)	m_0 (cm ³ /mole)	m_1 (cm ³ /mole K)	m_2 (cm ³ /mole K ²)	m_3 (cm ³ /mole K ³)	m_4 (cm ³ /mole K ⁴)
30	2.4–4.0	21.604	0.268 99	−0.024 294	0.009 859	0 ^a
28	2.4–4.0	21.9372	0.114 44	0.021 814	0.005 805	0 ^a
25	2.4–4.2	23.6319	−1.545 22	0.751 735	−0.134 615	0.010 212 9
20	2.2–4.0	23.8416	−1.071 46	0.496 186	−0.072 153	0.005 023 2
15	2.4–4.0	23.2088	0.474 72	−0.201 140	0.067 943	−0.004 713 4
10	2.4–3.9	25.7386	−1.626 81	0.727 395	−0.108 591	0.008 831 5
5	2.9–3.8	24.2154	1.051 02	−0.326 632	0.073 621	0 ^a

^a Fixed.

The isobars investigated by EM were rather close to those used by us; and since the expansion coefficient is only mildly dependent upon the pressure, no correction needed to be made for the slight differences in pressure. Only at the very highest of our pressures was it necessary to extrapolate slightly the measurements of EM in order to obtain a reasonable function for the molar volume. This extrapolation was done along isotherms, using smoothed and interpolated values of the expansion coefficient β_p . The extrapolated β_p data were fitted to a polynomial in T , and this function was integrated to obtain V (except for an additive constant which is not needed to calculate changes in ρ). The parameters for Eq. (4.3) are given in Table I.

Having obtained $(\Delta\rho)_s/\Delta T_s$, it remains to calculate

$$\beta_p \equiv -\rho^{-1} \left(\frac{\partial \rho}{\partial T} \right)_p = \lim_{\Delta T_s \rightarrow 0} \left(- \frac{(\Delta\rho/\rho)_s}{\Delta T_s} \right). \quad (4.4)$$

We used the density data along the λ line which are given by Kierstead,³⁰ and integrated our own $\Delta\rho/\Delta T$ data to get the temperature dependence of ρ . This temperature dependence is always quite small; and even as far as 0.02 K below T_λ , $(\rho_\lambda - \rho)/\rho_\lambda \lesssim 0.02$.

A curvature correction³¹ was applied to the data to correct for the difference between $(\Delta\rho/\Delta T)_p$ and $(\partial\rho/\partial T)_p$. This correction never exceeded 3%, and usually was less than 0.2%.

B. Errors

Random errors in our data for β_p very near T_λ are determined primarily by the resolution of 2×10^{-7} K in the measurement of ΔT_s . Errors due to the resolution of the ΔT_h measurements usually were negligible because ΔT_h was much larger than ΔT_s . Further away from T_λ ($|T_\lambda - T| \gtrsim 10^{-4}$ K), where temperature resolution was not a limitation, random errors were typically 0.2%. Random errors in $T_\lambda - T_s$ were somewhat larger than the temperature resolution because of the drifting of the sample-volume thermometer; but they never exceeded the larger of 1 μ K or 0.1% of $|T_s - T_\lambda|$.

Systematic errors in our data for β_p of as much as 3% could exist because of the uncertainties quoted by Elwell and Meyer for their molar volume measurements. We believe that all other sources of systematic errors are considerably smaller than this, and amount to no more than 0.5%. It should be emphasized that systematic errors in general do not influence the values of dimensionless critical-point parameters such as the exponents α and α' and the amplitude ratios A/A' and D/D' . The leading amplitudes A and A'

themselves, however, are subject to a 3% uncertainty.

V. RESULTS

A. Results for β_p

Measurements of the isobaric volume expansion coefficient β_p were made along nine isobars. The corresponding values of P_λ and T_λ are given in Table II. In addition to P_λ and T_λ for the nine isobars of our β_p measurements, Table II also contains results for three isobars along which β_p was not measured. The first two columns in this table give the pressure as determined from the two calibration methods of the capacitive pressure gauge, which were discussed in Sect. IIID. The third column gives our measured T_λ . We compare our λ -line parameters with those of Kierstead in the fourth column of the table, which contains $P_{\lambda K}$ determined from Eq. (3) of Ref. 30, using our T_λ . The difference between our P_λ and $P_{\lambda K}$ is never larger than reasonable estimates of errors due to uncertainties in P_λ and T_λ . The highest pressure given in the table corresponds to our determination of the intersection of the λ line and the solidification curve.

The range of

$$t \equiv T/T_\lambda - 1 \quad (5.1)$$

spanned by the data varied somewhat for different isobars. Near T_λ is usually extended to $|t| \cong 2 \times 10^{-5}$, and away from T_λ measurements for some pressures went as far as $|t| \cong 0.07$. Representative samples of the data are shown as a function of $\log_{10}|t|$ in Fig. 6. Altogether, 725 data points were obtained, and they are available in numerical form elsewhere.³²

TABLE II. λ -point parameters for the isobars.

$P_{\lambda 1}$ (bar)	$P_{\lambda 2}$ (bar)	T_λ^a (K)	$P_{\lambda K}$ (bar)
30.11 ± 0.06 ^b	...	1.7633 ^b	30.13 ^b
30.05 ± 0.06 ^c	...	1.7642	30.08
28.76 ± 0.06 ^c	28.71	1.7876	28.76
25.28 ± 0.09 ^c	25.22	1.8479	25.15
25.24 ± 0.06 ^c	25.13	1.8486	25.12
20.64 ± 0.09	20.55	1.9202	20.49
20.18 ± 0.06 ^c	20.21	1.9265	20.07
20.18 ± 0.09	20.12	1.9265	20.07
20.10 ± 0.06 ^c	20.06	1.9268	20.06
15.24 ± 0.06 ^c	15.23	1.9962	15.16
10.09 ± 0.06 ^c	10.05	2.0625	10.05
5.05 ± 0.06 ^c	5.06	2.1211	5.08

^a Uncertainty in T_λ is $\pm 1 \times 10^{-3}$ K.

^b Upper λ point.

^c Isobars on which β_p was measured.

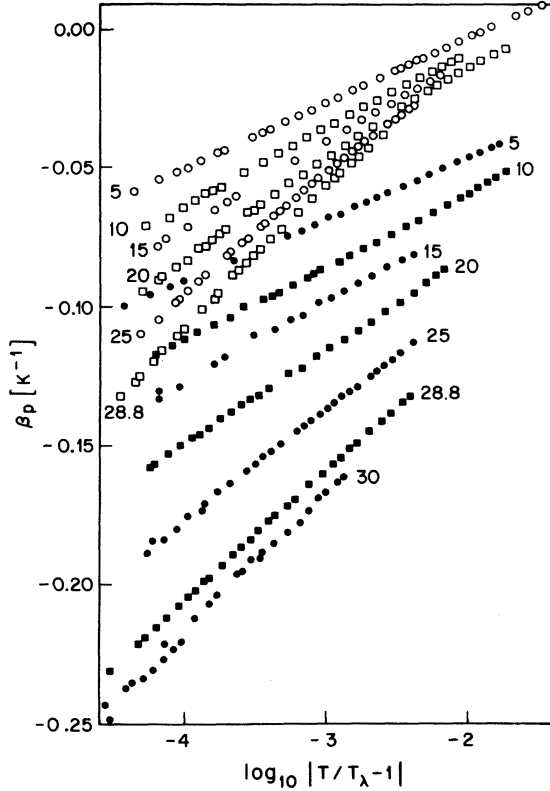


FIG. 6. Representative samples of the results for β_p on seven isobars, as a function of $\log_{10}|t|$. The numbers near each set of data points are the nominal pressures in bar. The solid symbols are for He II, and the open ones are for He I.

B. Closed-form representation of β_p

In order to facilitate thermodynamic calculations based on the measurements of β_p , it is convenient to have a closed-form expression for β_p which fits all the data within experimental uncertainties. As will be shown in detail below (Sec. VI), the equations

$$\beta_p = (A/\alpha)|t|^{-\alpha}(1 + D|t|^x) + B \quad (5.2a)$$

for $t > 0$ and

$$\beta_p = (A'/\alpha')|t|^{-\alpha'}(1 + D'|t|^{x'}) + B' \quad (5.2b)$$

for $t < 0$ with

$$\alpha = \alpha' = -0.026, \quad (5.3a)$$

$$x = x' = 0.5, \quad (5.3b)$$

$$A/A' = 1.11, \quad (5.3c)$$

$$D/D' = 1.11, \quad (5.3d)$$

and

$$B = B', \quad (5.3e)$$

serve this purpose for $|t| \leq 0.003$. Given this

TABLE III. Parameters for Eqs. (5.2), determined with the constraints given by Eqs. (5.3).

P (bar)	$-10^2 A'$ (K^{-1})	$-B'$ (K^{-1})	$-D'$
30.05	3.234	1.1932	0.408
28.76	2.976	1.1035	0.357
25.28	2.471	0.9232	0.294
25.24	2.452	0.9166	0.284
20.18	2.000	0.7531	0.233
20.10	1.990	0.7503	0.216
15.24	1.650	0.6251	0.174
10.09	1.437	0.5459	0.109
5.05	1.203	0.4542	0.080

form, we obtained from least-squares fits the values of A' , B' , and D' which are presented in Table III.

In order to obtain a reasonable interpolation between our pressures, the parameters in Table III were fitted to the polynomials

$$A' = a_0 + a_1 P + a_2 P^2 + a_3 P^3, \quad (5.4a)$$

$$B' = b_0 + b_1 P + b_2 P^2 + b_3 P^3, \quad (5.4b)$$

and

$$D' = d_0 + d_1 P + d_2 P^2 + d_3 P^3. \quad (5.4c)$$

The coefficients a_i , b_i , and d_i are given in Table IV. We will refer to the values of β_p given by Eqs. (5.2)–(5.4) and the coefficients in Table IV collectively as our reference values.

The deviations of the individual measurements from the reference values are shown as a function of $\log_{10}|t|$ in Fig. 7. Although occasionally slight systematic deviations are revealed by the data, the fit is generally quite good and the reference values usually give β_p to within $1 \times 10^{-3} K^{-1}$ provided $|t| \leq 0.003$.

C. Comparison with other results for β_p

The isobaric volume expansion coefficient along isobars near T_λ was measured previously by Ellwell and Meyer.¹¹ Since we used the results of EM well above T_λ (2.4–4.2 K) in our method of determining β_p (see Sec. IV A), it is particularly desirable as a check on the internal consistency of

TABLE IV. Parameters of Eqs. (5.4). The units are bar for P and K^{-1} for A' and B' . D' is dimensionless.

	i			
	0	1	2	3
$10^2 a_i$	-8.409	-0.8955	0.043 16	-0.001 320
$10^2 b_i$	-31.716	-3.3666	0.156 14	-0.004 677
$10^2 d_i$	-1.551	-1.410	0.050 68	-0.001 530

both sets of data to make a comparison of the results near T_λ . We have done this by subtracting our reference values of β_p from the measured values of EM^{33} for five of their isobars. This difference is shown as a function of $\log_{10}|t|$ in Fig. 8. It can be seen that within the scatter of the EM data there is good agreement with our data.

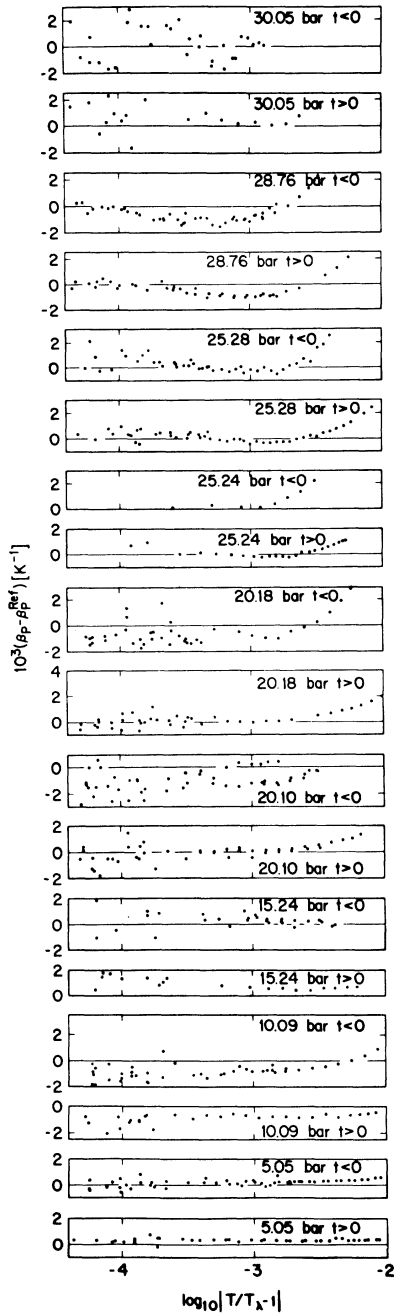


FIG. 7. Differences between our measured values of β_p , and the reference values given by Eqs. (5.2)–(5.4) with the coefficients in Table IV.

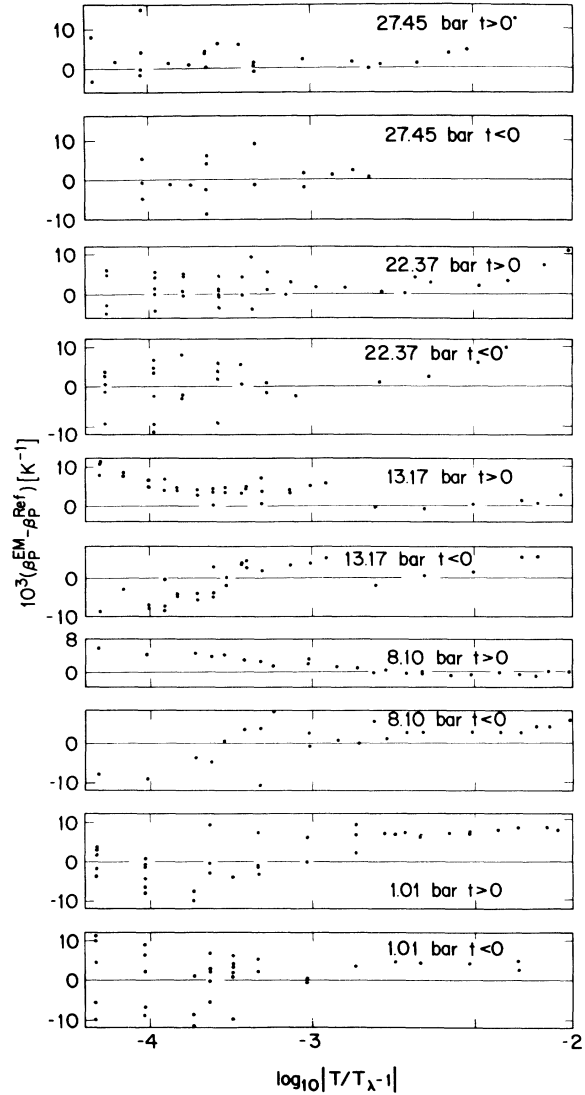


FIG. 8. Difference between the values of β_p measured by Elwell and Meyer (Ref. 33) and the reference values given by Eqs. (5.2)–(5.4) with the coefficients in Table IV. When comparing with Fig. 7, note the difference in the vertical scales.

Recently, a rather precise set of measurements of β_p at saturated vapor pressure has been made by Van Degrift and Pellam.³⁴ Although our results are only for $P \geq 5$ bar, it is interesting to compare those direct measurements with the extrapolation of our data to vapor pressure (0.05 bar) which is provided by Eqs. (5.2)–(5.4) and Table IV. We will not make a detailed comparison with the individual data points. Instead, we compare the coefficients of Eq. (5.2). With the constraints $\alpha = \alpha' = -0.026$, $x = x' = 0.5$, and $B = B'$, Van Degrift and Pellam obtained the results shown in the first row of Table V. Our extrapolated results, which are based on

TABLE V. Parameters of Eq. (5.2) at saturated vapor pressure. In each case, $\alpha = \alpha' = -0.026$, $x = x' = 0.5$, and $B = B'$ was assumed.

Source	A/A'	A' (K^{-1})	B' (K^{-1})	D'
Ref. 34	1.113	-0.00881	-0.324	-0.04
Eq. (5.4)	1.110 ^a	-0.00845	-0.319	-0.016
From C_p	1.110 ^a	-0.00909	-0.33 [^]	-0.009

^a Held fixed in the analysis.

the additional constraint $A/A' = 1.11$, are given in the second row of the table. The agreement for A/A' is excellent. Any difference in D' is insignificant because at vapor pressure D' is small and its uncertainty relatively large for both estimates. The differences in A' and B' , although only a few percent of A' and B' , are appreciable compared to the accuracy of β_p and indicate that our reference values should be used with some caution at pressures less than our lowest pressure of 5 bar. At vapor pressure, there is a roughly constant difference of $0.007 K^{-1}$ between our extrapolation and the values of β_p obtained by Van Degrift and Pellam, to be compared with typical uncertainties of $0.001 K^{-1}$ for direct measurements.

D. Comparison with the heat capacity at constant pressure

1. Vapor pressure

The heat capacity at constant pressure C_p near T_λ is an asymptotically linear function of β_p .³⁵ Specifically, along isobars

$$C_p = VT \left(\frac{\partial P}{\partial T} \right)_\lambda \beta_p + T \left(\frac{\partial S}{\partial T} \right)_t. \quad (5.5)$$

For $|t| \approx 3 \times 10^{-3}$, the parameters $T(\partial S/\partial T)_t$ and VT are essentially constant, and equal to their values $T_\lambda(\partial S/\partial T)_\lambda$ and $V_\lambda T_\lambda$ at T_λ . We used Eq. (5.5) and the known λ -line parameters at vapor pressure^{7, 30} to calculate the coefficients of Eq. (5.2) for β_p from those of a similar expression for the heat capacity at saturated vapor pressure.^{14, 35} The specific-heat parameters which we used were also based upon the constraints given by Eqs. (5.3). The results are given in the third row of Table V. They are consistent within experimental uncertainties with the thermal-expansion results of Van Degrift and Pellam. The yield values of β_p which differ by less than $0.001 K^{-1}$ from the direct measurements.

2. Higher pressures

At pressures higher than the saturated vapor pressure, the specific heat at constant pressure has not been measured directly; but it has been calculated via thermodynamic relations from the

measured heat capacity at constant volume C_v .⁷ These results for C_p had been interpreted to imply that the leading specific-heat amplitude ratio is pressure dependent.⁷ This interpretation is contrary to our present results for A/A' , based on β_p , to be discussed in Sec. VI D. A detailed comparison of C_p and β_p is therefore warranted. We have restricted this comparison to the pressure range $P \geq 5$ bar of the β_p data. For the pressures of the specific-heat measurements,⁷ we calculated C_p^β , using Eq. (5.5) and the reference values for β_p . We approximated $(\partial S/\partial T)_t$ by $(\partial S/\partial T)_\lambda$, and restricted the comparison to the range $|t| \leq 0.003$ where this approximation introduces a negligible error.⁷ For $(\partial P/\partial T)_\lambda$ we used the values given by Eq. (1) of Ref. 30, and $(\partial S/\partial T)_\lambda$ was obtained from Eqs. (4.16) and (4.17) of Ref. 7. The relative difference, in percent, between the measured C_p and that derived from β_p is shown in Fig. 9. For pressures up to 18.18 bar, this difference is generally less than 1%. For higher pressures, systematic departures occur between C_p and C_p^β . At 25.87 bar the differences are as large as 3% near $|t| \approx 10^{-3}$ and as large as 4.5% near $|t| \approx 10^{-4}$. This systematic difference, and in particular its dependence upon t , corresponds to the difference in the results for the amplitude ratio A/A' when this ratio is deduced either from β_p or from the high-pressure results for C_p .

The above comparison of C_p and C_p^β will be affected by errors in the direct measurement of C_v ,⁷ in the thermodynamic calculation necessary to obtain C_p from C_v ,⁷ in our own measurements of β_p , in the measurements of β_p at high temperatures by Elwell and Meyer¹¹ (to which our data are in effect normalized), and in the λ -line parameters $(\partial P/\partial T)_\lambda$ ³⁰ and $(\partial S/\partial T)_\lambda$.⁷ In view of this, we find it gratifying that the differences between C_p and C_p^β for $P \leq 18.18$ bar are generally less than 1%. In fact, even the larger differences at the higher pressures are only of the same size as reasonable estimates of the combined systematic errors (3–4%) that might be expected for all the experiments. However, the known possible systematic errors should be essentially independent of t ; and it is the t dependence of the difference between C_p and C_p^β that leads to the different conclusion regarding the amplitude ratio A/A' . We have no explanation for the cause of the t dependence at high P of $(C_p - C_p^\beta)/C_p^\beta$.

VI. COMPARISON WITH THEORETICAL PREDICTIONS

A. Theoretical predictions

The predictions of modern theories of critical phenomena that pertain to β_p are the same as those for C_p . This can be seen easily from Eq. (5.5). The coefficients $VT(\partial P/\partial T)_\lambda$ and $(\partial S/\partial T)_t$ in this

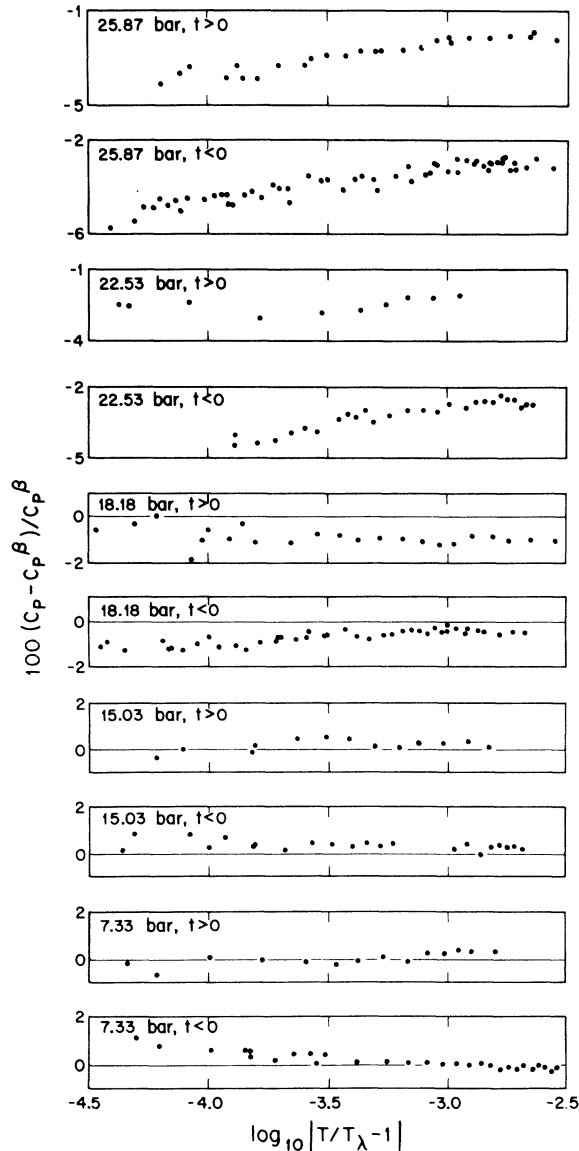


FIG. 9 Difference between the specific heat at constant pressure reported in Ref. 7, and that calculated via Eq. (5.5) from the reference values given by Eqs. (5.2)–(5.4) and the coefficients in Table IV.

equation can be shown to be less singular than β_P and C_P , and near T_λ approach a constant value with a leading temperature dependence given by terms of order t and $t^{1-\alpha}$.^{35,36} Therefore β_P is an asymptotically linear function of C_P and has the same exponents and amplitude ratios as C_P . Some of the amplitudes themselves, and any regular contributions, will of course be different; but the amplitudes and regular terms for C_P can be calculated from those of β_P and the known λ -line derivatives.

The predictions for C_P ,²⁻⁴ and thus for β_P , have

been discussed extensively in the recent literature,^{7,8,35} and we shall only summarize them here. They can be expressed readily in terms of the parameters defined by Eqs. (5.2a) and (5.2b). From scaling,² it is expected that

$$\alpha = \alpha'. \quad (6.1)$$

This result has been confirmed by the more recent renormalization-group theory of critical phenomena.⁴ In addition, it is expected from renormalization-group theory that

$$x = x', \quad (6.2)$$

and that⁹

$$B = B'. \quad (6.3)$$

The term $B = B'$ therefore represents a regular contribution to β_P .

The existence of confluent singularities, such as the terms $D|t|^x$ and $D'|t|^{x'}$ in Eqs. (5.2a) and (5.2b), has been established by experiment in the case of the superfluid density,³⁷ the specific heat,⁷ and the thermal conductivity³⁸ near T_λ . Their existence near critical points in general has been predicted from renormalization-group theory.³⁹ For the Ising model, these terms have been found also by high-temperature series expansions.⁴⁰ They may contribute significantly to experimental results, and therefore should be included in the data analysis. It is of course possible that D and D' are very small or vanish accidentally for a particular system.

In addition to the results Eqs. (6.1)–(6.3), it was predicted that certain dimensionless combinations of parameters are universal in the sense that they depend only upon very general symmetry properties of the system.³ These predictions have also been supported by the more rigorous results of renormalization-group theory.⁴ Specifically of interest here is the prediction that the exponents α and x , and the amplitude ratios A/A' , D/D' , and D'/a (a is the amplitude of the confluent singularity of the superfluid fraction ρ_s/ρ) should be independent of the pressure P along the λ line.

The earlier specific-heat measurements were consistent with the predictions Eqs. (6.1) and (6.2) and the universality of α and x . But when these theoretical results were imposed as constraints in the data analysis, those data yielded $B \neq B'$ at the higher pressures, contrary to Eq. (6.3). They also resulted in an amplitude ratio A/A' which depended upon P for $P \gtrsim 15$ bar (see Table XI of Ref. 7). This disagreement between experiment and theory provided the main motivation for the present work, and we shall see that the measurements of β_P are consistent with Eq. (6.3) and a universal A/A' . The inconsistencies between the measure-

ments of β_P and C_P have been discussed in Sec. V.

B. Method of analysis

In order to extract from the measurements parameters which can be compared with theoretical predictions, we used a nonlinear least-squares-fitting procedure which has been described elsewhere⁴¹ to fit pairs of data, separately for each isobar, to Eqs. (5.2a) and (5.2b). For weights we used $W_i = P_i^{-2}$, where our estimate of the probable error P_i of the i th data point was the larger of a 0.1% random error, or an error due to the 2×10^{-7} K temperature resolution.⁴¹ We did the analyses over the range $|t| \leq 0.003$. Although this choice is somewhat arbitrary, this range of t was wide enough to include a large number of precise data points, and yet confined $|t|$ to sufficiently small values to render negligible terms of order t , $|t|^{1-\alpha}$, and $|t|^{2\alpha}$ provided those terms have coefficients which are no larger than of order unity. Unless otherwise stated, results given below are based upon this temperature range.

The errors quoted below are standard errors. They do not include systematic errors; but we are not aware of any appreciable systematic errors in α , α' , x , x' , D , D' , A/A' , and D/D' . Specifically, we have ascertained that an error of 1×10^{-6} K in the determination of T_λ has a negligible effect upon the values of these parameters. The standard errors do, of course, include the correlation with all other parameters which were least-squares adjusted in a particular fit. For the same set of data, they therefore may be strongly dependent upon any constraints imposed upon the analysis.

It is perhaps worth mentioning that differences up to about two standard errors between two independent determinations of the same parameter, although they should be infrequent, may occur occasionally without necessarily implying any real inconsistency. In particular, the fact that a few of the points for $\alpha = \alpha'$, A/A' , and D/D' shown in Fig. 14 below have error bars which do not quite overlap with the mean values of these parameters should not be regarded either as an indication of the presence of significant unsuspected systematic errors, or of a departure from universality.

C. Analysis without higher-order singular terms

In the analysis of measurements pertaining to critical phenomena, the confluent singularities $D|t|^x$ and $D'|t|^{x'}$ which are contained in Eqs. (5.2a) and (5.2b) often are assumed to be absent. To a large extent, this is done because their inclusion in the analysis will increase the uncertainties of all other parameters, sometimes by as much as

an order of magnitude. Unless extremely precise and extensive data are available, the statistical errors which result from fits to Eqs. (5.2a) and (5.2b) or their equivalent can be larger than typical differences between parameters for systems which belong to different symmetry classes.

These large errors tend to imply that the measurements do not contain particularly useful information about the critical behavior of the system under investigation. We shall show in Sec. VID that a careful analysis of our results, incorporating reasonable constraints suggested by theory, yields significant information even when confluent singularities are included. However, it is the purpose of *this* section to demonstrate that their omission leads to serious conflicts with theoretical predictions.

When we fitted the data over the range $|t| \leq 3 \times 10^{-3}$ to Eqs. (5.2a) and (5.2b), setting $D = D' = 0$, we obtained values of α and α' which at all pressures were consistent with Eq. (6.1). We therefore imposed Eq. (6.1) as a constraint in a second set of least-squares fits, and obtained the values of $\alpha = \alpha'$ shown as open circles in Fig. 10. It is immediately clear that in this interpretation $\alpha = \alpha'$ is nonuniversal, varying from about 0.00 for P near 5 bar to +0.07 for P near 30 bar, with standard errors (shown by the bars in the figure) of

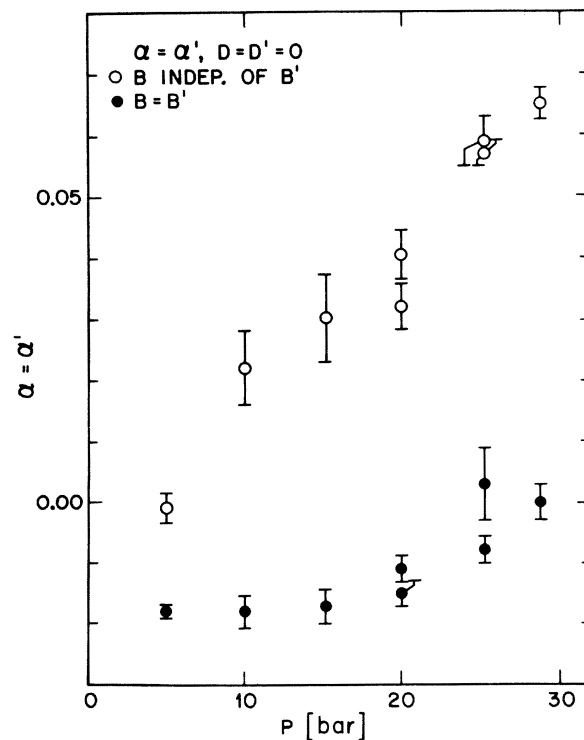


FIG. 10. Results for the leading exponent $\alpha = \alpha'$ of β_P based on fits of the data to pure power laws.

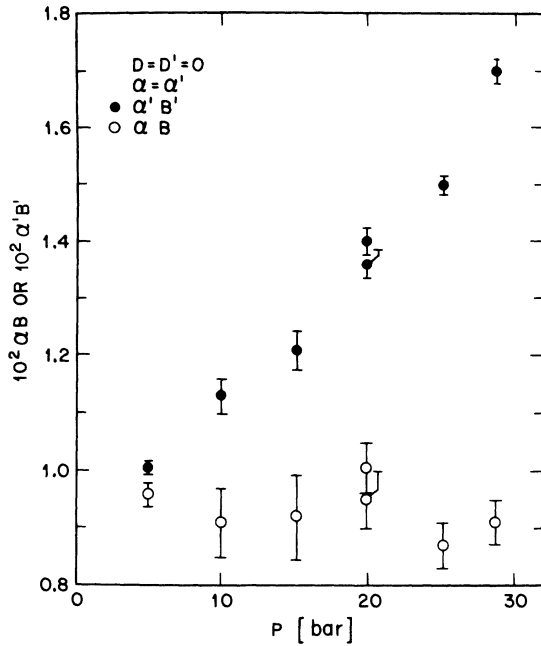


FIG. 11. Results for the constant terms $\alpha\beta$ and $\alpha\beta'$ [see Eq. (5.2)] based on fits of the data for β_P to pure power laws.

typically only ± 0.005 . The values of B and B' obtained from this fit are represented by the data in Fig. 11. Here we multiplied B and B' by α or α' because αB and $\alpha' B'$ depend much less upon α (note that B and B' diverge as α approaches zero, whereas αB and $\alpha' B'$ remain finite). It follows from Fig. 11 that Eq. (6.3) is not satisfied by the parameters obtained in this analysis.

Further manifestations of the difficulties are contained in the behavior of the amplitude ratio A/A' . We demonstrate this by plotting in Fig. 12 the parameter

$$\mathcal{P} \equiv (1 - A/A')/\alpha \quad (6.4)$$

as open circles. The behavior of this quantity has been discussed on the basis of renormalization-group predictions⁴² and experimental results for a number of systems,⁸ and it was found that \mathcal{P} is rather insensitive even to such relevant properties of the system as the spin dimensionality. From experiment, it was found that \mathcal{P} assumes values in the range 3.6–4.6 for systems with short-range forces. The open circles in Fig. 12, which pertain when B is independent of B' , all correspond to $\mathcal{P} < 0$, and therefore differ qualitatively from the behavior of other known systems near their critical points. Furthermore, although \mathcal{P} is predicted to be universal, it is found to be pressure dependent in this interpretation of our measurements.

Although the results in Fig. 11 clearly indicate that Eq. (6.3) is inconsistent with our data if $D = D' = 0$, we have nonetheless imposed $B = B'$ as a constraint in our analysis in order to study its effect upon the other parameters. For $\alpha = \alpha'$ we obtained the values shown as solid circles in Fig. 10. Although these results are not completely consistent with universality, their pressure dependence is a great deal less than that of the open circles. The corresponding values of \mathcal{P} are shown as solid circles in Fig. 12. They, too, are not quite universal; but they are much less pressure dependent than the results with B independent of B' . The values of \mathcal{P} are now largely in the expected range.

Although the imposition of the constraint $B = B'$ appears to have removed to a large extent the inconsistencies with the predicted universality, we hasten to add that the resulting fits of the data by Eqs. (5.2a) and (5.2b) with $D = D' = 0$ are statistically not satisfactory. We demonstrate this in Fig. 13, where we show the square roots of the variances σ which are obtained both with and without the constraint $B = B'$. At the highest pressure, σ is increased by a factor of 3.5 when $B = B'$ is imposed as a constraint. With the large number of data points available for these fits,

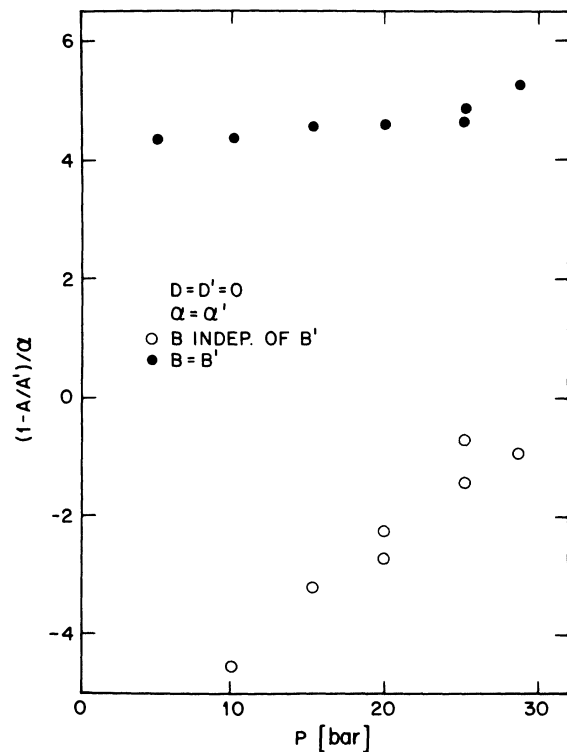


FIG. 12. Results for $\mathcal{P} = (1 - A/A')/\alpha$ based on fits of the data for β_P to pure power laws.

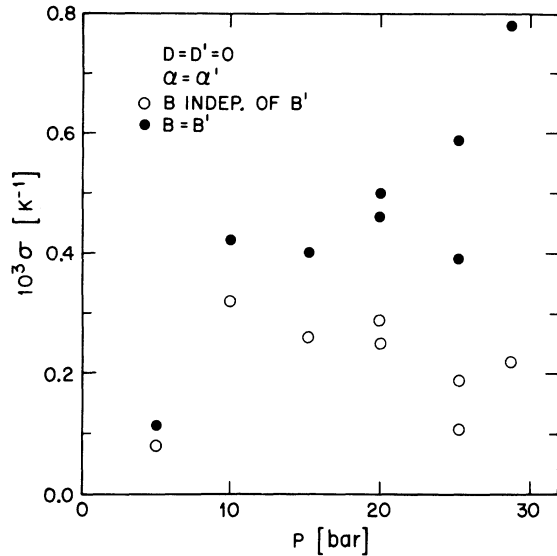


FIG. 13. Square root σ of the variance of the data for β_P based on fits to pure power laws.

even a change of only a few percent in σ must be regarded as significant.

D. Analysis with higher-order singular terms

We saw in Sec. VIC that an analysis of our data in terms of a pure power law leads to parameters which disagree with some of the theoretical predictions. In this section we will present the results which are obtained when confluent singularities are included in the analysis. We will find that the resulting parameters are consistent with pertinent theoretical results.

The task of obtaining useful information from the data by fitting to Eqs. (5.2a) and (5.2b) is a most difficult one because of the extremely high correlation between the ten parameters. Even if numerical techniques were developed to accomplish it, the standard errors for the parameters would be so large as to render their values meaningless for any comparison with theory. As was done before, particularly in the analysis of specific-heat measurements near magnetic phase transitions,^{8, 41, 43} we have therefore adopted some of the more general predictions of theory as constraints in the data analysis. The remaining free parameters were then least-squares adjusted, and can be compared with additional independent theoretical predictions. The approach thus is one of testing for consistency between experiment and some of the theoretical results on the one hand, and the remainder of the theoretical predictions on the other.

We adopted the value

$$x = x' = 0.5 \quad (6.5)$$

as a constraint in our analysis because the value of x is very poorly defined by thermal-expansion and specific-heat data. The value of x given by Eq. (6.5) is suggested by measurements of the superfluid density ρ_s ,³⁷ which should have the same correction exponent as β_P and C_P ,³⁹ and by high-temperature series expansions for the three-dimensional Ising model.⁴⁰ Additional support for this value, and for the weakness of the dependence of x upon the spin dimensionality n , comes from renormalization-group theory.³⁹ As a precaution, we repeated our calculations with $x = x' = 0.4$ and $x = x' = 0.6$. These values represent reasonable estimates for the lower and upper limits of x as determined from ρ_s or from the Ising-model series. We found that a change in x by 0.1 did not influence our conclusions.

Further, we assumed that $\alpha = \alpha'$. This constraint is predicted by theory and was statistically allowed by the data. We also assumed that $B = B'$. Although we saw in Fig. 11 that a pure-power-law analysis did not permit this constraint, the equality $B = B'$ was statistically allowed by the data when D and D' were permitted to differ from zero. With the above constraints [Eqs. (6.1), (6.3), and (6.5)], we fitted the data, separately for each isobar, to Eqs. (5.2a) and (5.2b) by least-squares adjusting simultaneously the six parameters α' , A' , A/A' , D' , D/D' , and B . Our main objective was of course to determine whether α' , A/A' , and D/D' were independent of pressure as predicted by theory. The results for these parameters are given in Fig. 14. It is evident from the statistical errors indicated by the bars on the points, and from the scatter, that the results are consistent with universal values for α' , A/A' , and D/D' . Weighted averages of the points for the various isobars are

$$\alpha = \alpha' = -0.026 \pm 0.004, \quad (6.6a)$$

$$A/A' = 1.112 \pm 0.022, \quad (6.6b)$$

and⁴⁴

$$D/D' = 1.29 \pm 0.25. \quad (6.6c)$$

From this analysis, we also obtain

$$\mathcal{P} = 4.32 \pm 0.19. \quad (6.6d)$$

When the same analysis was performed with the adopted value $x = x' = 0.4$, we still found $\alpha = \alpha'$, A/A' , and D/D' to be universal. Their average values were -0.029 ± 0.005 , 1.124 ± 0.027 , and 1.33 ± 0.22 . For \mathcal{P} we obtained 4.24 ± 0.20 . These results differ very little from Eqs. (6.6a)–(6.6d).

It is also important to obtain best estimates of the nonuniversal parameters A' , B' , and D' because they are useful in certain thermodynamic calculations, and because some of them can be combined with results from measurements of

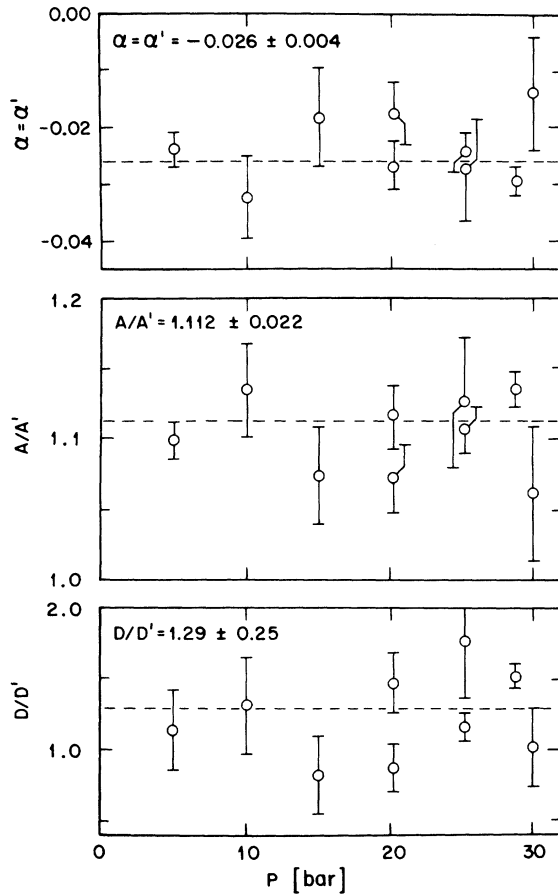


FIG. 14. Leading exponent $\alpha = \alpha'$, and the amplitude ratios A/A' and D/D' , of β_P based on fits to functions which include a confluent singularity [see Eq. (5.2)]. The correction exponent was assumed to have the value $x = x' = 0.5$. The dashed lines correspond to the weighted mean values given in the figure and by Eq. (6.6).

other properties of the fluid to form additional universal ratios or products. We therefore, somewhat arbitrarily, proceeded as follows. First, we imposed the constraints $x = x' = 0.5$ and $\alpha = \alpha' = -0.026$. When in addition we chose $A/A' = 1.112$, a slight trend of D/D' with pressure was observed. The values of D/D' remained within the error bars given in Fig. 14, however, and the pressure dependence can be attributed to the extreme sensitivity of D/D' at low P where D and D' are both very small to the choice of A/A' . We found that more nearly universal values of D/D' were obtained with the constraints $\alpha = \alpha' = -0.026$ and $A/A' = 1.110$. With this choice, the weighted average of D/D' was found to be 1.110. We adopted this set of universal values, given also by Eqs. (5.3a)–(5.3d), as constraints, and reanalyzed the data by least-squares ad-

justing A' , B' , and D' . The resulting parameters are given in Table III.

E. Comparison with specific heat

We know already that the results for $\alpha = \alpha'$, A/A' , and D/D' which follow from the specific-heat measurements⁷ differ from those obtained here from β_P when the pressure is greater than about 18 bar. But at lower pressures we would expect the two sets of measurements to give the same results. The comparison cannot be made immediately, however, because the specific heat had not been analyzed with the constraint $B = B'$. We therefore refitted the specific-heat data to the equivalent of Eqs. (5.2), using Eqs. (6.1), (6.3), and (6.5), as constraints. Appropriate weights⁷ were employed, and the temperature range was $|t| \leq 0.003$. This analysis is in every way equivalent to the one which led to the data in Fig. 14 and to Eqs. (6.6). We obtained the parameters in Table VI. All four parameters given there are consistent with universality for $P \leq 15.03$ bar. Over this pressure range, the mean values are

$$\alpha = \alpha' = -0.016 \pm 0.002, \quad (6.7a)$$

$$A/A' = 1.068 \pm 0.010, \quad (6.7b)$$

and

$$\wp = 4.21 \pm 0.06. \quad (6.7c)$$

These results can be compared with those derived from β_P and given by Eqs. (6.6). Both $\alpha = \alpha'$ and A/A' as derived from C_P differ somewhat from the corresponding results based on β_P ; but the differences are only slightly larger than the sums of the standard errors and are probably not significant. The values for \wp are more consistent with each other. In fact, even at the higher pressures where $\alpha = \alpha'$ and A/A' change appreciably, \wp remains rather close to its low-pressure value.

TABLE VI. Parameters $\alpha = \alpha'$, A/A' , \wp , and D/D' derived from the specific heat (Ref. 7) with the constraints Eqs. (6.1), (6.3), and (6.5). All data had $|t| \leq 0.003$.

P (bar)	$\alpha = \alpha'$	A/A'	\wp	D/D'
0.05	-0.016 ± 0.002	1.068 ± 0.006	4.15	...
1.65	-0.019 ± 0.007	1.081 ± 0.030	4.24	...
7.33	-0.014 ± 0.005	1.059 ± 0.020	4.17	1.2 ± 0.6
15.03	-0.015 ± 0.004	1.063 ± 0.016	4.28	0.6 ± 0.4
18.18	-0.038 ± 0.003	1.16 ± 0.02	4.34	1.39 ± 0.16
22.53	-0.069 ± 0.005	1.31 ± 0.03	4.53	1.74 ± 0.13
25.87	-0.045 ± 0.003	1.20 ± 0.02	4.57	1.37 ± 0.10

F. Comparison with superfluid fraction

Several of the parameters for β_p are expected to be related to those of ρ_s/ρ by scaling laws or universal ratios. For the leading exponents of these two properties, we have⁴⁵

$$\zeta = \frac{1}{3}(2 - \alpha'), \quad (6.8)$$

where ζ is defined by the equation

$$\rho_s/\rho = k |t|^\zeta (1 + a |t|^y). \quad (6.9)$$

The result quoted previously³⁷ for ζ was 0.67 ± 0.01 . This, and Eq. (6.6a) or Eq. (6.7a) for α' , clearly satisfy Eq. (6.8). However, a more detailed comparison is possible if it is assumed that α' and ζ are universal. In that case, the value of α' obtained here can be compared with the value of ζ derived from data at saturated vapor pressure. For that pressure, the thermodynamic parameters¹⁴ necessary to derive ρ_s/ρ from second-sound velocity measurements³⁷ are known more accurately than at higher pressures, and ρ_s/ρ can be obtained with higher precision. In addition, the measurements of ρ_s/ρ , C_p , and of β_p all show that the confluent singularities have small amplitudes at low pressure, and therefore the leading singularity can be measured more accurately. We reanalyzed the results³⁷ for ρ_s/ρ at vapor pressure, premitting k , ζ , a , and T_λ to be least-squares adjusted. We used data with $|t| \leq 0.01$. For y we chose the fixed values 0.5 and 0.3, and obtained the results given in Table VII. As always, the errors are standard errors. The change ΔT_λ of T_λ quoted in the table is the difference between the least-squares-adjusted value of T_λ and the value measured experimentally.³⁷ It is apparent that the measurements of ρ_s/ρ at vapor pressure define ζ with great accuracy, and that the value of ζ does not depend appreciably upon the exponent of the confluent singularity. We adopt the best estimate

$$\zeta = 0.675 \pm 0.001, \quad (6.10)$$

to be compared with

$$\frac{1}{3}(2 - \alpha') = 0.6753 \pm 0.0013 \quad (6.11a)$$

TABLE VII. Parameters for Eq. (6.9), obtained by refitting the results from Ref. 37 at vapor pressure with the constraints $y=0.5$ and $y=0.3$. ΔT_λ is in K.

y	0.5	0.3
ζ	0.6750 ± 0.0005	0.6747 ± 0.0008
k	2.548 ± 0.010	2.540 ± 0.019
a	0.007 ± 0.021	0.010 ± 0.017
$10^6 \Delta T_\lambda$	0.7 ± 0.2	0.6 ± 0.2

which follows from Eq. (6.6a) or

$$\frac{1}{3}(2 - \alpha') = 0.6720 \pm 0.0007 \quad (6.11b)$$

which follows from Eq. (6.7a). Clearly the agreement is very good in either case, although the value of α' derived from β_p is more consistent with ζ and scaling. The above comparison of α' and ζ constitutes the only experimental confirmation of a scaling law with parameters which are determined by fitting to functions which include confluent singularities.

In addition to the leading exponent, one can in principle compare also the correction exponent; for it is expected from renormalization-group theory³⁹ that $x=y$. None of the data define x or y with sufficient accuracy to provide a very stringent test; but within the fairly large uncertainties the measurements are consistent with the prediction.

A third pair of parameters that can be compared are the amplitudes D' and a of the confluent singularities. On the basis of general renormalization-group considerations, their ratio D'/a is expected to be universal.⁴⁶ Results for D' are quoted in Table III and are given by Eq. (5.4c) and the parameters in Table IV. Values of a as a function of P had been obtained previously³⁷ only by simultaneously least-squares adjusting k , ζ , and a . These results are subject to sizable experimental errors because of the high correlation between ζ and a . They are reasonably consistent with a universal ratio D'/a , however. A more detailed test of the universality of D'/a can be obtained by fitting the measurements of ρ_s/ρ to Eq. (6.9), with Eqs. (6.10) for ζ as an additional constraint. Such a fit yielded the values of a given in Table VIII. Here the results at vapor pressure are omitted because D' and a are so small that they have not been determined with meaningful accuracy. Also shown in the table are the values of D' at the pressures of the ρ_s measurements as computed from Eq. (5.4c). The corresponding ratios D'/a are given in the fourth column of Table VIII. There is a monotonic trend of D'/a with pressure which, if real, would be contrary to the expected

TABLE VIII. Amplitudes of confluent singularities for $\beta_p(D')$ and $\rho_s/\rho(a)$.

P (bar)	a	D'	D'/a
7.27	0.43	-0.09	-0.21
12.13	0.77	-0.14	-0.18
18.06	1.22	-0.20	-0.16
24.10	2.00	-0.28	-0.14
29.09	2.98	-0.37	-0.13

universal behavior. However, both D' and a are very sensitive to slight changes in ζ , α , or x . In addition, we have not explored the effect on D' and a of neglecting additional terms of higher order than $D'|t|^{x'}$ and $a|t|^{y'}$. Therefore we cannot be sure that the values of D'/a in Table VIII are sufficiently free from systematic errors to be inconsistent with universality. It is encouraging that D'/a varies by only about a factor of 1.6, whereas D' and a separately varied by factors of 4 and 7, respectively.

Finally, it should be possible to compare the leading amplitude of ρ_s/ρ with that of β_P via the predicted two-scale-factor universality of Stauffer, Ferer, and Wortis.⁵ However, we feel that the leading amplitudes of ρ_s and of β_P are subject to sizable systematic errors. The uncertainty of A is of the order of 3%, and that of k for P greater than vapor pressure is perhaps as large as 6 or 8% because both C_P and the entropy S must be known in order to derive k from the measured second-sound velocity. In view of these uncertainties, it seems premature to reexamine the Stauffer-Ferer-Wortis ratio at this time.

VII. SUMMARY AND CONCLUSION

We described in this paper a new method of measuring with high temperature and pressure resolution the isobaric thermal-expansion coefficient β_P of liquid ^4He near the superfluid transition. We presented experimental results for β_P in the vicinity of T_λ for nine isobars. It was possible to represent these measurements by a single equation, both as a function of temperature and pressure.

The results were compared with other results for the expansion coefficient,^{11,34} and with the heat capacity at constant pressure C_P .^{7,14} Except for C_P at pressures greater than about 15 bar, all the results are consistent with each other, and differences do not exceed reasonable estimates of possible systematic or random errors of the various experimental results. For P greater than 18 bar, there exist systematic differences between the previous results for C_P and estimates of C_P based upon β_P . These differences slightly exceed reasonable *a priori* estimates of the possible systematic errors of the data, and become as large as $4\frac{1}{2}\%$ at the highest pressure and closest to T_λ . For P less than 18 bar they do not exceed 1% however. The origin of the problem at high P is not known at present. It is worth noting, however, that the results for C_P were not obtained directly; instead, they were calculated via thermodynamic relations from measurements of the heat capacity at constant volume C_V .⁷ It is desirable to further

investigate the discrepancy by performing direct measurements of C_P .

Our results for β_P were compared in detail with theoretical predictions based on scaling,² universality,³ and on the renormalization-group theory of critical phenomena.⁴ For this purpose, we first fitted the data to pure power laws. This analysis yielded exponents and amplitude ratios which were dependent upon the pressure. Such a pressure dependence is contrary to theoretical predictions based on universality arguments³ and the renormalization-group theory.⁴ This analysis also yielded values for the additive constant B above T_λ [see Eq. (6.2)] which differed from the constant B' below T_λ . This also is contrary to the predictions of renormalization-group theory.⁹

Since the data analysis based upon pure power laws resulted in serious conflicts with theoretical predictions, we reanalyzed the measurements by fitting them to functions which, in addition to the leading singularity also included a confluent singularity [see Eq. (5.2)]. This analysis yielded parameters which were consistent with the theoretically predicated result $B=B'$. We then imposed the prediction $B=B'$ as a constraint in the analysis. This constraint reduced the statistical errors for the remaining free parameters very appreciably. We found that the leading exponents $\alpha=\alpha'$, the leading amplitude ratio A/A' , and the amplitude ratio D/D' of the confluent singularities all were independent of pressure within their statistical errors, as expected from theory,^{3,4} We conclude that agreement between theoretical predictions and the experimental results is obtainable, but only if the contribution to β_P from confluent singularities is taken into consideration. Our best estimates for $\alpha=\alpha'$, A/A' , and D/D' are given by Eq. (6.6).

The exponents and amplitude ratios of β_P were compared with those derived from C_P . For this purpose, the specific-heat results⁷ were reanalyzed in a manner consistent with the analysis of the expansion-coefficient data. For $P \leq 15$ bar, the data for C_P yielded values of $\alpha=\alpha'$ and A/A' which differed only very slightly from those derived from β_P [see Eq. (6.7)]. Although the small differences which do exist are slightly larger than the statistical errors derived from the data, they probably should not be regarded as significant. In any event, they are much smaller than typical differences in these parameters for systems which belong to different universality classes.⁷ For higher pressures, both $\alpha=\alpha'$ and A/A' as derived from C_P are pressure dependent and inconsistent with the values obtained from β_P . The specific heat did not yield values of D/D' with meaningful accuracy.

We also compared some of the parameters of β_P

with those of the superfluid density ρ_s . For this purpose, we reanalyzed the ρ_s data at vapor pressure³⁷ in a manner which is more consistent with our analysis of β_p . The result $\zeta = 0.675 \pm 0.001$ and our value $\alpha = \alpha' = -0.026 \pm 0.004$ rather accurately obey the scaling law⁴⁵ $\zeta = \frac{1}{3}(2 - \alpha')$. This comparison of ζ and α' is the first experimental confirmation of a scaling law with parameters which are derived by fitting data to functions which include confluent singularities. We also examined the ratio D'/a . Here D' and a are the amplitudes of the confluent singularities of β_p and ρ_s , respectively. This ratio is expected to be independent of the pressure.⁴⁶ We found that D'/a varied by about a factor of 1.6 over our pressure range; but we were unable to show that this pressure dependence exceeded systematic errors in D'/a . In any event, D' and a by themselves change a great deal more with pressure and vary by a factor of 4 and 7, respectively, over our range of P .

ACKNOWLEDGMENT

We are grateful to A. Kornblit for his help with the data analysis.

APPENDIX A: FOUNTAIN-PRESSURE EFFECTS

For $T_s < T_\lambda$, the pressure P_h in the hot volume will differ from the sample pressure P_s by an increment due to the fountain pressure P_f across the capillary (see also Sec. IV A). Since P_f depends upon T_s , the pressure P_h will also depend upon T_s because P_s is held constant. Therefore changes in fountain pressure ΔP_f which are associated with sample temperature changes ΔT_s will result in hot-volume density changes $\delta(\Delta\rho)_h$ in addition to the density changes that would occur if conditions in the hot volume, too, were isobaric. The change $\delta(\Delta\rho)_h$ was neglected in our data analysis. The relative error in $\beta_{p,s}$ due to this approximation is given by

$$\delta\beta_{p,s}/\beta_{p,s} = \delta(\Delta\rho)_h/(\Delta\rho)_h. \quad (\text{A1})$$

It can be estimated by considering

$$\left(\frac{d\rho}{dT}\right)_h - \left(\frac{\partial\rho}{\partial T}\right)_{P,h} = \left(\frac{\partial\rho}{\partial P}\right)_{T,h} \left(\frac{dP}{dT}\right)_h. \quad (\text{A2})$$

We have

$$\frac{\delta(\Delta\rho)_h}{(\Delta\rho)_h} = \left(\frac{\partial\rho}{\partial P}\right)_{T,h} \left(\frac{dP}{dT}\right)_h / \left(\frac{d\rho}{dT}\right)_h. \quad (\text{A3})$$

When the left of this equation is small,

$$\frac{\delta(\Delta\rho)_h}{(\Delta\rho)_h} \cong \frac{(\partial\rho/\partial P)_{T,h}}{(\partial\rho/\partial T)_{P,h}} \frac{dP_f}{dT_h}, \quad (\text{A4})$$

where we used $dP_h = dP_f$. Using the relation $(\partial\rho/\partial P)_T/(\partial\rho/\partial T)_P = -(\partial T/\partial P)_\rho$ and Eq. (A1), one

gets from Eq. (A4)

$$\frac{\delta\beta_{p,s}}{\beta_{p,s}} \cong - \left(\frac{\partial T}{\partial P}\right)_{\rho,h} \frac{dP_f}{dT_h}. \quad (\text{A5})$$

With Eq. (2.1) in the form

$$\frac{dT_h}{dT_s} = - \frac{N_s \beta_{p,s}}{N_h \beta_{R,h}}, \quad (\text{A6})$$

one finally obtains

$$\frac{\delta\beta_{p,s}}{\beta_{p,s}} \cong \frac{N_h \beta_{p,h}}{N_s \beta_{p,s}} \left(\frac{\partial T}{\partial P}\right)_{\rho,h} \frac{dP_f}{dT_s}. \quad (\text{A7})$$

For the purpose of estimating the size of the error in $\beta_{p,s}$, we use $N_h/N_s \cong 0.1$, $\beta_{p,h} \cong -\beta_{p,s}$ (under most conditions of the experiment $|\beta_{p,s}| > \beta_{p,h}$), and $(\partial T/\partial P)_{\rho,h} \approx 2 \times 10^{-7}$ cm² K/dyn.⁴⁷ We find approximately

$$\left| \frac{\delta\beta_{p,s}}{\beta_{p,s}} \right| \approx 2 \times 10^{-8} \frac{dP_f}{dT_s} \quad (\text{A8})$$

with P_f in dyn cm⁻².

There are no measurements of the fountain pressure across a capillary similar to ours in the vicinity of T_λ ; and there is also no rigorous quantitative theoretical prediction. An upper limit for P_f is given by the London equation,⁴⁸ and can be written as

$$P_f \leq \rho S(T_\lambda - T_s). \quad (\text{A9})$$

Departures from the equality increase with increasing capillary diameter. Our diameter is rather large (0.01 cm), and we expect our P_f to be much less than that given by Eq. (A9). One finds³⁵ that $\rho S \approx 2 \times 10^6$ erg cm⁻³ K⁻¹ along the λ line, and that $|\delta\beta_{p,s}/\beta_{p,s}| \ll 0.04$.

A more realistic, but empirical, estimate can be obtained from the rule of Allen and Reekie.⁴⁹ These authors used the proportionality between the pressure gradient in a channel or tube and the associated heat current which is given by linear two-fluid hydrodynamics, and proposed that this proportionality should hold approximately also for large heat currents when dissipative processes occur. For a cylindrical geometry, one has⁵⁰

$$P_f = 8\eta l Q / \pi a^4 \rho S T, \quad (\text{A10})$$

where η is the normal-fluid viscosity, l is the length of the tube, Q is the heat current, and a is the tube radius. For $T \gtrsim 2$ K and at vapor pressure, measurements on a slit geometry by Keller and Hammel⁵¹ have shown that the rule of Allen and Reekie holds remarkably well, although at lower temperatures substantial departures from the rule exist for large temperature gradients.^{50,51} When departures do occur, the rule seems to yield an overestimate of P_f .⁵¹ On the basis of

previous measurements in a geometry¹⁵ similar to ours the heat current in our capillary can be estimated to be $Q \cong 9 \times 10^4 t^{1.077}$ erg/sec. Here $t \equiv (T_\lambda - T_s)/T_\lambda$. With $\eta \approx 2 \times 10^{-5}$ P, $l = 4$ cm, and

$a = 5 \times 10^{-3}$ cm, one obtains $P_f = 540 t^{1.077}$ dyn/cm², and $dP_f/dT_s \approx -190$ dyn/cm²K for $t \cong 0.01$. The error in $\beta_{P,s}$, given by Eq. (A8), is obviously negligible.

*Present address: Los Alamos Scientific Laboratory, University of California, Los Alamos, N. M. 87544.

†Part of the work by Guenter Ahlers done while this author was on temporary leave from Bell Laboratories at the Kernforschungsanlage Jülich.

¹For a recent review of experiments near the superfluid transition, see G. Ahlers, in *The Physics of Liquid and Solid Helium*, edited by K. H. Bennemann and J. B. Ketterson (Wiley, New York, 1976), Pt. I, Chap. 2; and F. Pobell, in *Liquid and Solid Helium, Proceedings of the European Physical Society Topical Conference*, edited by C. G. Kuper, S. G. Lipson, and M. Revzen (Wiley, New York, 1975), p. 357.

²B. Widom, *J. Chem. Phys.* **43**, 3898 (1965); C. Domb and D. L. Hunter, *Proc. Phys. Soc. Lond.* **86**, 1147 (1965); L. P. Kadanoff, *Physics (N.Y.)* **2**, 263 (1966); A. Z. Patashinskii and V. L. Pokrovskii, *Zh. Eksp. Teor. Fiz.* **50**, 439 (1966) [*Sov. Phys.-JETP* **23**, 292 (1966)]; R. B. Griffiths, *Phys. Rev.* **158**, 176 (1967); J. W. Essam and M. E. Fisher, *J. Chem. Phys.* **39**, 842 (1963).

³Early statements of the hypothesis of universality may be found in M. E. Fisher, *Phys. Rev.* **16**, 11 (1966); P. G. Watson, *J. Phys. C* **2**, 1883 (1969); **2**, 2158 (1969); D. Jasnow and M. Wortis, *Phys. Rev.* **176**, 739 (1968). More recent references are L. P. Kadanoff, in *Critical Phenomena, Proceedings of the International School "Enrico Fermi,"* edited by M. S. Green (Academic, New York, 1971); R. B. Griffiths, *Phys. Rev. Lett.* **24**, 1479 (1970); D. D. Betts, A. J. Guttmann, and G. S. Joyce, *J. Phys. C* **4**, 1994 (1971); D. Stauffer, M. Ferer, and M. Wortis, *Phys. Rev. Lett.* **29**, 345 (1972); K. G. Wilson and J. Kogut, *Phys. Rep. C* **12**, 76 (1974).

⁴K. G. Wilson, *Phys. Rev. B* **4**, 3174 (1971); **4**, 3184 (1971). For a review of the application of renormalization-group theory to critical phenomena, see K. G. Wilson and J. Kogut, *Phys. Rep. C* **12**, 76 (1974); M. E. Fisher, *Rev. Mod. Phys.* **46**, 597 (1974).

⁵D. Stauffer, M. Ferer, and M. Wortis, *Phys. Rev. Lett.* **29**, 345 (1972); A. Aharony, *Phys. Rev. B* **9**, 2107 (1974); P. C. Hohenberg, A. Aharony, B. I. Halperin, and E. D. Siggia, *Phys. Rev. B* **13**, 2986 (1976).

⁶See, for instance, J. M. H. Levelt Sengers, *Physica (Utr.)* **73**, 73 (1974); *J. Phys. Chem. Ref. Data* (to be published).

⁷G. Ahlers, *Phys. Rev. A* **8**, 530 (1973).

⁸See, for instance, G. Ahlers and A. Kornblit, *Phys. Rev. B* **12**, 1938 (1975).

⁹E. Brézin (private communication). See also Ref. 8 for a discussion of the equality $B = B'$.

¹⁰K. H. Mueller, F. Pobell, and G. Ahlers, *Phys. Rev. Lett.* **34**, 513 (1975); in *Liquid and Solid Helium, Proceedings of the European Physical Society Topical Conference*, edited by C. G. Kuper, S. G. Lipson, and M. Revzen (Wiley, New York, 1975), p. 57.

¹¹D. L. Elwell and H. Meyer, *Phys. Rev.* **164**, 245 (1967);

D. L. Elwell, Ph.D. thesis (Duke University, 1967) (unpublished).

¹²G. C. Straty and E. D. Adams, *Rev. Sci. Instrum.* **40**, 1393 (1969).

¹³L. E. De Long, O. G. Symko, and J. G. Wheatley, *Rev. Sci. Instrum.* **42**, 147 (1971).

¹⁴G. Ahlers, *Phys. Rev. A* **3**, 696 (1971).

¹⁵G. Ahlers, *Phys. Rev. Lett.* **22**, 54 (1969).

¹⁶G. Ahlers, *Phys. Rev. Lett.* **21**, 1159 (1968).

¹⁷G. Ahlers, *Phys. Rev.* **171**, 275 (1968).

¹⁸Cryocal, Inc., 1371 Avenue E, Riviera Beach, Fla. 33404.

¹⁹G. G. Ihas and F. Pobell, *Phys. Rev. A* **9**, 1279 (1974).

²⁰Bourdon Tube Co., Inc., Newtown, Conn. 06470. We used gauge No. CMM7435 (16-in. diam, 0–32 atm absolute).

²¹1% metal film resistors, normal electronics grade, with a temperature coefficient of 50 ppm/°C at room temperature.

²²Singer (Gertsch Operation), 3211 S. LaCienega Blvd., Los Angeles, Calif. 90016, model RT-9 Ratiotran.

²³Princeton Applied Research Corp. P. O. Box 2565, Princeton, N. J., 08540, model HR-8 or 124A.

²⁴General Radio Co., Concord, Mass., 01742, model 1616 capacitance bridge.

²⁵Linear Research, P. O. Box 9308, San Diego, Calif. 92109, model LR-130 temperature controller.

²⁶See, for instance, E. M. Forgan, *Cryogenics* **14**, 207 (1974).

²⁷We replaced the original thermometer on the sample volume by a new one, but encountered the same problem with drifts thereafter. We do not know the source of the difficulty, but were able to adequately compensate for it in the present measurements.

²⁸H. van Dijk, M. Durieux, J. R. Clement, and J. K. Logan, *Natl. Bur. Std. (U.S.) Monograph* **10** (U.S. GPO, Washington, D. C., 1960).

²⁹Datametries, 340 Fordham Road, Wilmington, Mass. 01887, Barocel type 1014A electronic manometer.

³⁰H. A. Kierstead, *Phys. Rev.* **162**, 153 (1967).

³¹See, for instance, E. F. Westrum, Jr., G. T.

Furukawa, and J. P. McCullough, in *Experimental Thermodynamics*, edited by J. P. McCullough and D. W. Scott (Plenum, New York, 1968), Vol. 1, Chap. 5, p. 187.

³²See AIP document No. PAPS PLRBA-14-2096-10 for 10 pages of tabulated data. Order by PAPS number and journal reference from American Institute of Physics, Physics Auxiliary Publication Service, 335 East 45th Street, New York, N. Y. 10017. The price is \$ 1.50 for each microfiche (98 pages), or \$ 5 for photocopies of up to 30 pages with \$ 0.15 for each additional page over 30 pages. Airmail additional. Make checks payable to the American Institute of Physics. This material also appears in *Current Physics Microfilm*, the monthly microfilm edition of the complete set of

- journals published by AIP, on the frames immediately following this journal article.
- ³³D. L. Elwell, in Ref. 11.
- ³⁴C. T. Van Degrift and J. R. Pellam, in *Proceedings of the Thirteenth International Conference on Low Temperature Physics*, edited by K. D. Timmerhaus, W. J. O'Sullivan, and E. F. Hammel (Plenum, New York, 1974), Vol. 1, p. 343; and to be published; C. T. Van Degrift, Ph.D. thesis (University of California at Irvine, 1974) (unpublished), and private communication.
- ³⁵See, for instance, G. Ahlers, in Ref. 1.
- ³⁶In principle, these coefficients are permitted to be more singular at isolated points on a λ line. On the basis of experiment [Refs. 30 and 35, and G. Ahlers, *J. Low Temp. Phys.* 7, 361 (1972)], such points are believed not to exist along the λ line of ^4He .
- ³⁷D. S. Greywall and G. Ahlers, *Phys. Rev. Lett.* 28, 1251 (1972); *Phys. Rev. A* 7, 2145 (1973).
- ³⁸G. Ahlers, in *Proceedings of the Twelfth International Conference on Low Temperature Physics*, edited by E. Kanda (Academic, Japan, 1971), p. 21.
- ³⁹F. J. Wegner, *Phys. Rev. B* 5, 4529 (1972); E. Brézin, J. C. LeGuillou, and J. Zinn-Justin, *Phys. Rev. D* 8, 2418 (1973); A. D. Bruce and A. Aharony, *Phys. Rev. B* 10, 2078 (1974); J. W. Swift and M. K. Grover, *Phys. Rev. A* 9, 2579 (1974).
- ⁴⁰D. M. Saul, M. Wortis, and D. Jasnow, *Phys. Rev. B* 11, 2571 (1975).
- ⁴¹A. Kornblit and G. Ahlers, *Phys. Rev. B* 8, 5163 (1973).
- ⁴²M. Barmatz, P. C. Hohenberg, and A. Kornblit, *Phys. Rev. B* 12, 1947 (1975).
- ⁴³A. Kornblit and G. Ahlers, *Phys. Rev. B* 11, 2678 (1975).
- ⁴⁴The small difference between the value of D/D' given here and that quoted in Ref. 10 is due to the fact that additional data have been obtained since the previous publication.
- ⁴⁵B. D. Josephson, *Phys. Lett.* 21, 608 (1966).
- ⁴⁶F. J. Wegner, in Ref. 39; and B. I. Halperin (private communication). The universality of D'/a has been predicted also by D. D. Betts (unpublished) on the basis of an extended universality hypothesis.
- ⁴⁷R. W. Hill and O. V. Lounasmaa, *Philos. Trans. R. Soc. Lond.* 252, 357 (1960).
- ⁴⁸H. London, *Nature* 142, 612 (1938).
- ⁴⁹J. F. Allen and J. Reekie, *Proc. Cambridge Philos. Soc.* 35, 114 (1939).
- ⁵⁰D. F. Brewer and D. O. Edwards, *Philos. Mag.* 6, 1173 (1961).
- ⁵¹W. E. Keller and E. F. Hammel, *Ann. Phys. (N.Y.)* 10, 202 (1960). See particularly their Fig. 15, where Q is a nearly linear function of P_f for temperatures near T_λ .